

AD 746186

DEPARTMENT OF CIVIL ENGINEERING  
DIVISION OF STRUCTURES AND MECHANICS

UNIVERSITY OF WASHINGTON  
SEATTLE, WASHINGTON

FREQUENCY DOMAIN ANALYSIS FOR THE TENSION  
IN A TAUT MOORING LINE

by

S.-T. Hong

July 1972

Technical Report No. 3M72-1

Prepared for

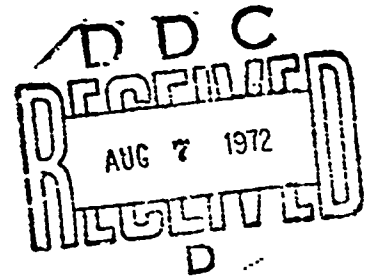
OFFICE OF NAVAL RESEARCH  
OCEAN SCIENCE AND TECHNOLOGY DIVISION

Contract No. N000 14-67-A-0103-0014

Task No. NR083-012

Reproduction in whole or in part is permitted for any purpose of the United  
States Government. Approved for public release: Distribution Unlimited.

Reproduced by  
NATIONAL TECHNICAL  
INFORMATION SERVICE  
U.S. Department of Commerce  
Springfield, MA 01101



UNCLASSIFIED

Security Classification

## DOCUMENT CONTROL DATA - R &amp; D

(Security classification of title, body of abstract and indexing annotation must be entered when the overall report is classified)

1. ORIGINATING ACTIVITY (Corporate author) Department of Civil Engineering University of Washington (Through the Department of Seattle, Washington 98195 Oceanography)		2a. REPORT SECURITY CLASSIFICATION Unclassified	
		2b. GROUP	
3. REPORT TITLE Frequency Domain Analysis for the Tension in a Taut Mooring Line			
4. DESCRIPTIVE NOTES (Type of report and inclusive dates)			
5. AUTHOR(S) (First name, middle initial, last name) Sheu-Tien Hong			
6. REPORT DATE July 1972		7a. TOTAL NO. OF PAGES 77	7b. NO. OF REFS 21
8a. CONTRACT OR GRANT NO. N000 14-67-A-0103-0014		9a. ORIGINATOR'S REPORT NUMBER(S) SM72-1	
b. PROJECT NO. NR 083-012			
c.		9b. OTHER REPORT NO(S) (Any other numbers that may be assigned this report)	
d.			
10. DISTRIBUTION STATEMENT Approved for public release; distribution unlimited.			
11. SUPPLEMENTARY NOTES		12. SPONSORING MILITARY ACTIVITY Office of Naval Research Code 480	
13. ABSTRACT <p>This report provides a frequency domain analysis for the tension in long, taut mooring lines. The analysis considers both the steady state and dynamic conditions. Computer programs for the analysis of both cases are included.</p> <p>The requirement of linearity of the system evident in frequency domain analysis calls for linearization of such features as drag and internal damping. These matters are dealt with and the order of practical relevance discussed in a quantitative manner.</p>			

UNCLASSIFIED

Security Classification



TABLE OF CONTENTS	i
LIST OF FIGURES	ii
1. Introduction	1
2. Steady State Mooring Line Tension	3
3. Dynamic Mooring Line Tension	5
4. Design Considerations	21
5. Summary and Conclusions	28
APPENDIX A. Hydrodynamic Drag on Mooring Rope and Buoy	30
APPENDIX B. Discussion of Model Simplifications	38
APPENDIX C. Program STEADY	48
APPENDIX D. Program DYN SIN	55
APPENDIX E. Program DYN RAN	65
REFERENCES	76

## LIST OF FIGURES

Fig. 1	Free Body of a Mooring Line Element	3
Fig. 2	Idealized Mooring Line and Free Body Diagram of the Rope Element	8
Fig. 3	Free Body Diagram of the $k^{\text{th}}$ Package	11
Fig. 4	Graphs of $P\eta(\eta)$ , the Probability Distribution of the Heights of Maxima ( $\eta = y_p/u_y$ ) for Different Values of the Width $\epsilon$ of the Energy Spectrum	17
Fig. 5	A Zero-Mean, Gaussian, Stationary Random Signal	18
Fig. 6	Density Curve of the Maximum Peak Values	20
Fig. 7	The Effect of Damping Sources on the Frequency Response Functions of Mooring Line Force at Buoy	22
Fig. 8	The Effect of Damping Sources on the Frequency Response Functions of Mooring Line Force at Anchor	23
Fig. 9	The Effect of Tangential Hydrodynamic Drag Coefficient on the Frequency Response Functions of Mooring Line Force at Buoy	24
Fig. 10	Variation of the Variance of Dynamic Force Along the Mooring Line	25
Fig. 11	The Effect of Tangential Hydrodynamic Drag Coefficient on the Variation of Dynamic Force Along the Mooring Line	26
Fig. 12	The Effect of Frequency on the Variation of Dynamic Force Along the Mooring Line	26
Fig. 13	The Effect of Significant Wave Height on Dynamic Force Along the Mooring Line	26
Fig. A.1	Dependence of Drag Coefficient on Reynolds Number for Flows Normal and Tangential to Smooth and Rough Circular Cylinders	31
Fig.A.2	Dimensions of the Discus Buoy Used in this Study	35
Fig.A.3	Detail of the Buoy Hull	36
Fig.B.1	Comparative Wave Spectra from FFWM and Monster Buoy	39
Fig.B.2	Vibrating Stretched String Under Lateral Loading	40

## 1. INTRODUCTION

For the convenience of analysis, mooring line tension under the excitation of wind, wave and current may be divided into a steady state component and a dynamic component. The steady state mooring line tension is defined as the force induced by the mooring line geometry, gravity, average current and average wind, and the dynamic tension by wave and wind gusts. The steady state analysis has been treated extensively and the solution can be achieved in a relatively small amount of computer time. The dynamic analysis has not been developed to the point where a low cost computer program with good accuracy is available. The works of Paquette and Henderson,<sup>(2)</sup> Wilson and Garbaccio,<sup>(3)</sup> Reid,<sup>(4)</sup> Kaplan and Ralf,<sup>(5)</sup> Nath,<sup>(6)</sup> and Brainard<sup>(7)</sup> are typical of the studies of the dynamic response of single point moorings made in recent years.

Extensive reviews of the literature on the response of various cable systems under hydrodynamic loading are presented by Casarella and Parsons.<sup>(1)</sup>

A time domain analysis is most desirable for the solution of mooring line tension under random waves. The solution technique may be divided into two types: the digital computer approach through the use of the method of characteristics and the analog computer approach. The latter has been discussed in Kaplan and Raff.<sup>(5)</sup> The basic formulation of the field equations based on the method of characteristics was presented by Reid<sup>(4)</sup> and Nath,<sup>(8)</sup> and a digital computer program was developed by Nath.<sup>(6)</sup>

By supplying a simulated random wave<sup>(9)</sup> as the excitation to the buoy system, the random stress history at any point of the mooring line can be obtained. Based on the simulated wave and the stress history, the autocovariance function, the cross covariance function, stress peak distribution curve, and the average frequency can be derived. However, each of the steps, i.e. wave simulation, solution program and statistical analysis, involves extensive

computer time. The high cost and special knowledge required by this method may make it too expensive for normal design use.

In the light of the difficulties encountered in a complete time domain analysis, it is necessary to search for an analytical solution in the frequency domain in order that the dynamic response of a buoy system under random input can be performed in a small amount of computer time. Additionally, little knowledge of time-series analysis is needed. However, the frequency domain analysis is only applicable to a linear structural system, and consequently the non-linear system has to be linearized.

The behavior of the mooring system is heavily dependent on the hydrodynamic drags on the surface buoy and the mooring rope. As will be shown later, the tangential mooring line hydrodynamic drag is a major damping factor in the response of a deep sea mooring line subject to oscillatory longitudinal motion at one end. However, neither theoretical solutions nor experimental data are available for the estimation of the tangential drag coefficient of a rope under oscillating motion.

A review of the drag coefficients on the mooring rope and the surface buoy is presented in Appendix A.

## 2. STEADY STATE MOORING LINE TENSION

In two dimensional analysis, the steady state tension in the mooring line is defined as the force induced by geometry, gravity, and the coplanar average current and wind. This is considered the best approximation of the mean stress in the mooring line subject to a definite combination of wind, wave and current, and the coplanar assumption gives a conservative solution.

Consider the two dimensional free body of an elemental length of the mooring line as shown in Fig. 1.

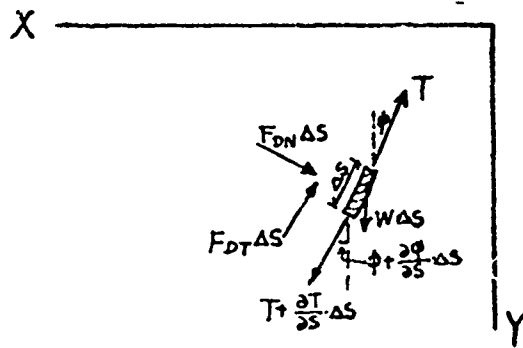


Figure 1. Free Body of a Mooring Line Element

The equilibrium equations in normal and tangential directions, after neglecting the second order terms, are

$$(F_{DN} + W \sin \phi) \Delta s = T \Delta \phi \quad (1)$$

and

$$(F_{DT} - W \cos \phi) \Delta s = \Delta T \quad (2)$$

where  $W$  is the weight of the rope in water per unit length,

$F_{DN}$  and  $F_{DT}$  are as in Equation (A.2) and (A.3).

Treating the mooring line as a series of finite chords, the solution of (1) and (2) can be approximated by incremental numerical integration. The computer program is presented in Appendix C.

The program can handle the compound mooring line, made of wire rope and



synthetic line, with instrument packages. The program capacity and rate of convergence will be discussed in Appendix C.

### 3. DYNAMIC MOORING LINE TENSION

#### 3.1 Model Simplifications

For reasons stated in the Introduction, the dynamic mooring line tension problem is solved using the frequency domain approach. Since the frequency domain analysis is only applicable to a linear structural system, the buoy system has to be simplified.

The basic assumptions of the buoy model considered in this work are as follows:

(1) The buoy is a surface follower buoy so that the buoy response spectrum can be considered to be the same as the wave spectrum.

(2) The mooring line is taut and can be treated as a straight string. The dynamic force in the mooring line due to the horizontal movement of the surface buoy under the action of wave and fluctuating wind is negligible compared to that due to the vertical motion of the buoy.

(3) The tangential hydrodynamic drag on the mooring line, which is proportional to velocity squared, can be linearized through a principle of equivalent linearization.

(4) The internal damping of the mooring ropes is linear and the dynamic stress strain relation under sinusoidal motion is given by

$$\sigma = (E_1 + iE_2)\epsilon$$

Depending on the material behavior under dynamic loading, the linear damping material may be represented by several types of mathematical models. One of the models listed in Table 1 may be used to describe the behavior of mooring lines and the models are incorporated into the solution program DYNSIN and DYNRAN as described in the Appendices.

(5) Stress due to strumming is neglected.

The validity of the first assumption depends on the type of buoy under consideration. This is discussed in Appendix B. The computer program developed for the dynamic analysis of the mooring line is based on the assumption that the buoy is a surface follower type, e.g. discus buoy. For buoys other than the surface follower type, a transfer function between the wave spectrum and the buoy response spectrum has to be established before a valid result may be expected. However, the assumption will provide an upper bound solution to the dynamic tension of the mooring line provided the natural frequency of the heave motion of the buoy is far from the effective wave frequency. In the case of a stationary buoy, e.g. spur buoy, the dynamic tension may be considered as negligible. The second, fourth and fifth assumptions introduce negligible error, as discussed in Appendix B. The error due to the linearization of the hydrodynamic drag will depend on the degree of non-linearity. The distortion of the result may be negligible at a low sea state and significant at a high sea state.

No error bound is available, and the accuracy can only be checked by experimental data as discussed in Appendix B.

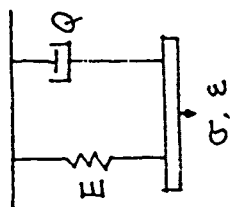
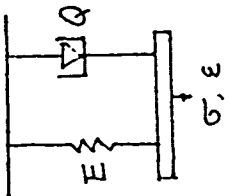
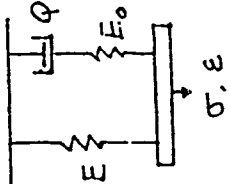
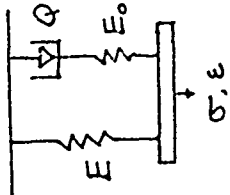
### 3.2 Dynamic Mooring Line Tension Under Sine Wave

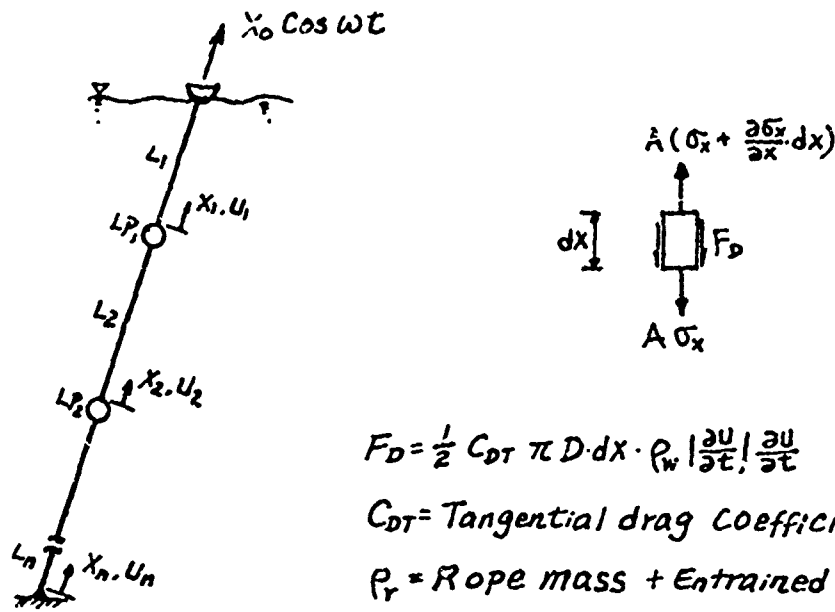
A deep sea mooring line with instrument packages inserted in it is idealized as Fig. 2.

The equilibrium condition of the free body, after neglecting the second order terms, leads to:

$$A \frac{\partial \sigma_x}{\partial x} - \frac{1}{2} C_{DT} \pi D \rho_w \left| \frac{\partial u}{\partial t} \right| \cdot \frac{\partial u}{\partial t} - \rho_r A \cdot \frac{\partial^2 u}{\partial t^2} = 0 \quad (3)$$

Table 1. Linear Damping Material Models

Model No.	1	2	3	4
Model name	Voigt Type linear dashpot model	Voigt Type li- near rate-inde- pendent model	Three parameter rate dependent Maxwell model	Three parameter rate independent Maxwell model
Model Description				
Constitutive equation	$\sigma = E\epsilon + Q \frac{d\epsilon}{dt}$	$\sigma = E\epsilon + \frac{Q}{E_0} \frac{d\sigma}{dt}$	$\sigma + \frac{Q}{E_0} \frac{d\sigma}{dt} = E\epsilon + (E+E_0) \frac{Q}{E_0} \frac{d\epsilon}{dt}$	$\sigma + \frac{1}{\omega} \frac{Q}{E_0} \frac{d\sigma}{dt} = E\epsilon + (E+E_0) \frac{1}{\omega} \frac{Q}{E_0} \frac{d\epsilon}{dt}$
E1	E	E	$E + \frac{E_0 \omega^2 (Q/E_0)^2}{1 + \omega^2 (Q/E_0)^2}$	$E + \frac{E_0 \omega^2}{E_0^2 + Q^2}$
E2	Q	Q	$\frac{\omega Q}{1 + \omega^2 (Q/E_0)^2}$	$\frac{E_0^2 Q}{E_0^2 + Q^2}$
D	$\frac{\pi \omega Q}{E^2 + Q^2 \omega^2} \sigma_0^2$ or $\pi Q \omega \epsilon_0^2$	$\frac{\pi Q}{E^2 + Q^2} \sigma_0^2$ or $\pi Q \epsilon_0^2$	$\frac{\pi \omega Q}{E^2 + (E+E_0)^2 \frac{\omega^2 Q^2}{E_0^2}} \sigma_0^2$ or $\frac{\pi \omega Q}{1 + \omega^2 (Q/E_0)^2} \epsilon_0^2$	$\frac{\pi Q E_0^2}{E^2 E_0^2 + (E+E_0)^2 Q^2} \sigma_0^2$ or $\frac{\pi F_0^2 Q}{F_0^2 + Q^2} \epsilon_0^2$
Remarks	$\sigma = (E+E_0)\epsilon$ ; $\sigma_0, \epsilon_0$ are stress, strain amplitude respectively, E, $E_0$ and Q are material constants			



$$F_D = \frac{1}{2} C_{DT} \pi D \cdot dx \cdot \rho_w \left| \frac{\partial u}{\partial t} \right| \frac{\partial u}{\partial t}$$

$C_{DT}$  = Tangential drag Coefficient

$\rho_r$  = Rope mass + Entrained water

Fig. 2- Idealized Mooring Line and Free Body Diagram of the Rope Element

Introducing the relation  $\sigma = (E_1 + iE_2)\epsilon = (E_1 + iE_2) \frac{\partial u}{\partial x}$

into Equation (3) and dividing by  $AE_1$ , then

$$\frac{\partial^2 u}{\partial x^2} + i \frac{E_2}{E_1} \frac{\partial^2 u}{\partial x^2} - \frac{C_{DT} \pi D \rho_w}{2AE_1} \left| \frac{\partial u}{\partial t} \right| \cdot \frac{\partial u}{\partial t} - \frac{\rho_r}{E_1} \frac{\partial^2 u}{\partial t^2} = 0 \quad (4)$$

Equation (4) may be linearized to

$$\frac{\partial^2 u}{\partial x^2} + i\tau \frac{\partial^2 u}{\partial x^2} - C_{DR} \frac{\partial u}{\partial t} - \frac{1}{a^2} \frac{\partial^2 u}{\partial t^2} = 0 \quad (5)$$

where

$$\tau = \frac{E_2}{E_1}, \quad a^2 = \frac{E_1}{\rho_r} \quad \text{and } C_{DR} \text{ is the equivalent linear damping parameter as}$$

derived in (B.27).

Separating variables in the form

$$U(x,t) = X(x) \cdot e^{i\omega t} \quad (6)$$

where  $X(x)$  is complex, then the spatial part of Equation (5) becomes

$$(1 + i\tau)X_1 x + \left(\frac{\omega^2}{a^2} - i\omega C_{DR}\right)X = 0 \quad (7)$$

This has the solution

$$X(x) = (R_1 + iI_1) \sin(\alpha + i\beta)x + (R_2 + iI_2) \cos(\alpha + i\beta)x \quad (8)$$

where  $R_1, I_1, R_2, I_2$  are real constants to be determined from boundary and continuity conditions, and

$$\alpha = \left[ \frac{\left[ \left( \frac{\omega}{a} \right)^2 - \tau C_{DR} \omega \right] + \left\{ \left[ \left( \frac{\omega}{a} \right)^2 - \tau C_{DR} \omega \right]^2 + \left[ C_{DR} \omega + \tau \left( \frac{\omega}{a} \right)^2 \right]^2 \right\}^{\frac{1}{2}}}{2(1 + \tau^2)} \right]^{\frac{1}{2}} \quad (9)$$

$$\beta = - \left[ \frac{- \left[ \left( \frac{\omega}{a} \right)^2 - \tau C_{DR} \omega \right] + \left\{ \left[ \left( \frac{\omega}{a} \right)^2 - \tau C_{DR} \omega \right]^2 + \left[ C_{DR} \omega + \tau \left( \frac{\omega}{a} \right)^2 \right]^2 \right\}^{\frac{1}{2}}}{2(1 + \tau^2)} \right]^{\frac{1}{2}} \quad (10)$$

The values of  $a, \tau$  and  $C_{DR}$  will depend on the material model and the material constants. They are constants for the two parameter models and frequency dependent functions for the three parameter models.

The relation between  $E_1, E_2$  and the material constants for various models are shown in Table 1.

The displacement is now

$$U(x,t) = [(R_1 + iI_1) \sin(\alpha + i\beta)x + (R_2 + iI_2) \cos(\alpha + i\beta)x] e^{i\omega t} \quad (11)$$

The strain is

$$\frac{\partial U(x,t)}{\partial x} = [(R_1 + iI_1)(\alpha + i\beta) \cos(\alpha + i\beta)x - (R_2 + iI_2)(\alpha + i\beta) \sin(\alpha + i\beta)x] e^{i\omega t} \quad (12)$$

and the stress is

$$\sigma_x = (E_1 + iE_2) \frac{\partial U}{\partial x} \quad (13)$$

Considering only the real parts and rearranging gives the displacement

$$U(x,t) = A_1 \cos \omega t + A_2 \sin \omega t = U_A(x) \cos(\omega t + \phi_1) \quad (14)$$

where

$$A_1 = R_1 SCx + I_1 CSx + R_2 CCx + I_2 SSx$$

$$A_2 = - (R_1 CSx + I_1 SCx - R_2 SSx + I_2 CCx)$$

$$U_A = (A_1^2 + A_2^2)^{\frac{1}{2}}$$

$$SSx = \sin \alpha x \sinh \beta x$$

$$SCx = \sin \alpha x \cosh \beta x$$

$$CSx = \cos \alpha x \sinh \beta x$$

$$CCx = \cos \alpha x \cosh \beta x$$

the strain

$$\frac{\partial u}{\partial x} = B_1 \cos \omega t + B_2 \sin \omega t = \epsilon_A(x) \cos (\omega t + \phi_2) \quad (15)$$

where

$$B_1 = (-R_2 \alpha + I_2 \beta) SCx + (R_2 \beta + I_2 \alpha) CSx + (R_1 \alpha - I_1 \beta) CCx + (I_1 \alpha + R_1 \beta) SSx$$

$$B_2 = (R_2 \beta + I_2 \alpha) SCx - (-R_2 \alpha + I_2 \beta) CSx - (I_1 \alpha + R_1 \beta) CCx + (R_1 \alpha - I_1 \beta) SSx$$

$$\epsilon_A = (B_1^2 + B_2^2)^{\frac{1}{2}}$$

and the mooring line tension

$$\sigma_x = C_1 \cos \omega t + C_2 \sin \omega t = \sigma_A \cos (\omega t + \phi_3) \quad (16)$$

where

$$C_1 = A[R_1(E_1 \alpha CCx + E_1 \beta SSx - E_2 \beta CCx + E_2 \alpha SSx)$$

$$+ I_1(-E_1 \beta CCx + E_1 \alpha SSx - E_2 \beta CCx - E_2 \alpha SSx)$$

$$+ R_2(-E_1 \alpha SCx + E_1 \beta CSx + E_2 \beta SCx + E_2 \alpha CSx)$$

$$+ I_2(E_1 \beta SCx + E_1 \alpha CSx + E_2 \alpha SCx - E_2 \beta CSx)]$$

$$\begin{aligned}
C_2 = & -A[R_1(E_1\beta CCx - E_1\alpha SSx + E_2\beta CCx + E_2\beta SSx) \\
& + I_1(E_1\alpha CCx + E_1\beta SSx - E_2\beta CCx + E_2\alpha SSx) \\
& + R_2(-E_1\alpha SCx + E_1\beta CSx + E_2\beta SCx + E_2\alpha CSx) \\
& + I_2(E_1\beta SCx + E_1\alpha CSx + E_2\alpha CSx - E_2\beta CSx)
\end{aligned}$$

The free body diagram of a package is illustrated in Fig. 3. The equilibrium equation of the package is

$$-A_K(\sigma_{X_K})_{X_K=0} + A_{K+1}(\sigma_{X_{K+1}})_{X_{K+1}=L_{K+1}} + C_{DPK} \frac{\partial u}{\partial t} + PM_K \frac{\partial^2 u}{\partial t^2} = 0 \quad (17)$$

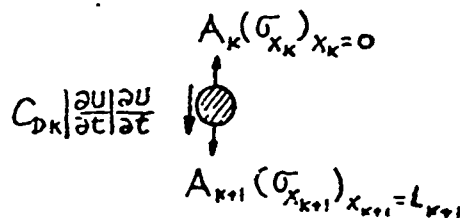


Fig. 3. Free Body of the  $k^{th}$  Package

where

$$C_{DPK} = \frac{4\rho_w C_{DK} A_K U_A \omega}{3} \text{ as derived in (B.23)}$$

$C_{DK}$  is the dimensionless drag coefficient of the  $k^{th}$  package.

$PM_K$  is the mass of the  $k^{th}$  package plus the virtual mass. The boundary and continuity conditions are:

$$\begin{aligned}
(1) \quad & U_1(L_1, t) = X_0 \cos \omega t \\
(2) \quad & PM_1 \ddot{U}_{P1} + C_{DP1} \dot{U}_{P1} - A_1(\sigma_{x1})_{x1=0} + A_2(\sigma_{x2})_{x2=0} = 0 \\
(3) \quad & U_1(0, t) = U_{P1}(t) = U_2(L_2, t) \\
(4) \quad & PM_2 \ddot{U}_{P2} + C_{DP2} \dot{U}_{P2} - A_2(\sigma_{x2})_{x2=0} + A_3(\sigma_{x3})_{x3=0} = 0 \\
& \vdots \\
(2n-1) \quad & U_{n-1}(0, t) = U_{P_{n-1}}(t) = U_n(L_n, t) \\
(2n) \quad & U_n(0, t) = 0
\end{aligned} \quad (18)$$



$$\text{From } U_n(0,t) = 0, \quad R_{2n} = I_{2n} = 0$$

By using  $U_p(t) = U_k(0,t)$  and substituting (14), (15) into (18), the equation can be presented in the matrix form shown on page 13, where

$$K_{12}^K = \sin \alpha_K L_K \cosh \beta_K L_K$$

$$K_{21}^K = \cos \alpha_K L_K \sinh \beta_K L_K$$

$$K_{11}^K = \sin \alpha_K L_K \sinh \beta_K L_K$$

$$K_{22}^K = \cos \alpha_K L_K \cosh \beta_K L_K$$

$$P_{11}^K = -A_K E_{1K} \alpha_K + A_K E_{2K} \beta_K$$

$$P_{12}^K = A_K E_{1K} \beta_K + A_K E_{2K} \alpha_K$$

$$P_{13}^K = -PM_K \omega^2$$

$$P_{14}^K = -C_{DPK} \omega$$

$$P_{15}^K = A_{K+1} (E_1)_{K+1} (\alpha_{K+1} K_{22}^{K+1} + \beta_{K+1} K_{11}^{K+1}) + A_{K+1} (E_2)_{K+1} (\alpha_{K+1} K_{11}^{K+1} - \beta_{K+1} K_{22}^{K+1})$$

$$P_{16}^K = A_{K+1} (E_1)_{K+1} (\alpha_{K+1} K_{11}^{K+1} - \beta_{K+1} K_{22}^{K+1}) + A_{K+1} (E_2)_{K+1} (-\alpha_{K+1} K_{22}^{K+1} - \beta_{K+1} K_{11}^{K+1})$$

$$P_{17}^K = A_{K+1} (E_1)_{K+1} (\beta_{K+1} K_{21}^{K+1} - \alpha_{K+1} K_{12}^{K+1}) + A_{K+1} (E_2)_{K+1} (\alpha_{K+1} K_{12}^{K+1} + \beta_{K+1} K_{21}^{K+1})$$

$$P_{18}^K = A_{K+1} (E_1)_{K+1} (\alpha_{K+1} K_{21}^{K+1} + \beta_{K+1} K_{12}^{K+1}) + A_{K+1} (E_2)_{K+1} (\alpha_{K+1} K_{12}^{K+1} - \beta_{K+1} K_{21}^{K+1})$$

$$P_{21}^K = -(A_K E_{1K} \beta_K + A_K E_{2K} \alpha_K)$$

$$P_{22}^K = -A_K E_{1K} \alpha_K + A_K E_{2K} \beta_K$$

$$P_{23}^K = C_{DFK} \omega$$

$$P_{24}^K = -PM_K \omega^2$$

$$P_{25}^K = A_{K+1} (E_1)_{K+1} (\beta_{K+1} K_{22}^{K+1} - \alpha_{K+1} K_{11}^{K+1}) + A_{K+1} (E_2)_{K+1} (\alpha_{K+1} K_{22}^{K+1} + \beta_{K+1} K_{11}^{K+1})$$

$$P_{26}^K = A_{K+1} (E_1)_{K+1} (\alpha_{K+1} K_{22}^{K+1} + \beta_{K+1} K_{11}^{K+1}) + A_{K+1} (E_2)_{K+1} (\alpha_{K+1} K_{11}^{K+1} - \beta_{K+1} K_{22}^{K+1})$$

$$P_{27}^K = A_{K+1} (E_1)_{K+1} (-\alpha_{K+1} K_{21}^{K+1} - \beta_{K+1} K_{12}^{K+1}) + A_{K+1} (E_2)_{K+1} (\beta_{K+1} K_{21}^{K+1} - \alpha_{K+1} K_{12}^{K+1})$$

$$P_{28}^K = A_{K+1} (E_1)_{K+1} (\beta_{K+1} K_{21}^{K+1} - \alpha_{K+1} K_{12}^{K+1}) + A_{K+1} (E_2)_{K+1} (\alpha_{K+1} K_{21}^{K+1} + \beta_{K+1} K_{12}^{K+1})$$

[illegible]

By solving (19), values of  $R_1, I_1, R_2, I_2, \dots, R_{2n-1}, I_{2n-1}$  can be obtained and the displacement, strain and stress can be computed from (14), (15), and (16).

A computer program to obtain the equivalent linear damping coefficient and solve Equation (19), written in Fortran IV and coded in CDC 6400, is presented in Appendix D.

### 3.3 Dynamic Mooring Line Tension Under Random Waves

The random vibration solution to a linear system has been well developed. The random response of a non-linear system is usually treated by either linearizing the non-linear system or generating a response history by means of a simulated random loading.

The linearization technique for random vibration is much more difficult than that for the cyclic vibration, and the accuracy can only be verified by experiment. However, for reasons stated previously, a linearized system will be employed in this work.

#### 3.3.1 System Linearization for Random Analysis

Equation (4) may be rewritten in the form

$$\left(1 + i \frac{E_2}{E_1}\right) \frac{\partial^2 u}{\partial x^2} - C_R \frac{\partial u}{\partial t} - \frac{\rho_r}{E_1} \frac{\partial^2 u}{\partial t^2} + E = 0 \quad (20)$$

where

$$E = C_R \frac{\partial u}{\partial t} - \frac{C_{DT} \pi D \rho_w}{A E_1} \left| \frac{\partial u}{\partial t} \right| \frac{\partial u}{\partial t}$$

$U$  is a random variable, and  $E$  is an error vector.

The linearization of Equation (20) may be accomplished by determining the value of  $C_R$  which would minimize the square of the error vector  $E$  and then deleting  $E$  from the equation, thus

$$\frac{\partial \{E^2\}}{\partial C_R} = \left\{ \left[ C_R \dot{U} - \frac{C_{DT} \pi D \rho_w}{2 A E_1} |\dot{U}| \dot{U} \right] \dot{U} \right\} = 0$$

and

$$C_R = \frac{C_{DT} \cdot \pi \cdot D \cdot \rho_w}{2AE_1} \cdot \frac{\{|\dot{U}| \cdot \dot{U}^2\}}{\{\dot{U}^2\}} \quad (21)$$

where  $\{\cdot\}$  represents the expectation.

Assuming  $U(t)$  is a Gaussian process with zero mean, ensures that  $\dot{U}$  is also a Gaussian process with zero mean with density function

$$p_U(\dot{U}) = \frac{1}{\sqrt{2\pi} \sigma_{\dot{U}}} e^{-\frac{\dot{U}^2}{2\sigma_{\dot{U}}^2}} \quad (22)$$

Substituting Equation (22) into (21) and performing the integration, gives

$$C_R = \frac{C_{DT} \pi D \rho_w}{2AE_1} \cdot \frac{\sqrt{8}}{\pi} \frac{\sigma_{\dot{U}}^3}{\sigma_{\dot{U}}^2} \quad (23)$$

Equation (21) may also be obtained by equating the average power dissipation in both systems.

This discussion is so far limited to a definite point in the rope to find a value of  $C_R$  for the whole rope; an averaging process must be carried out by integrating over the whole length:

$$\begin{aligned} C_R &= \frac{C_{DT} \cdot \pi \cdot D \cdot \rho_w}{2AE_1} \cdot \frac{\int_0^L \{|\dot{U}| \cdot \dot{U}^2\} dx}{\int_0^L \{\dot{U}^2\} dx} \\ &= \frac{C_{DT} \cdot \pi \cdot D \cdot \rho_w}{2AE_1} \cdot \frac{\sqrt{8}}{\pi} \frac{\int_0^L \sigma_{\dot{U}}^3 dx}{\int_0^L \sigma_{\dot{U}}^2 dx} \end{aligned} \quad (24)$$

Repeating this procedure allows the equivalent linear damping coefficient for the instrument package in (17) to be represented by

$$C_{DP} = \frac{C_{DN} A \rho_w}{2} \cdot \frac{\sqrt{8}}{\pi} \cdot \sigma_{\dot{U}} \quad (25)$$

### 3.3.2 Solution Technique

The spectral approach is a convenient tool for obtaining the statistics of the response process of a linear system under random loading. The spectral approach employs the equation,

$$S_y(\omega) = |H(\omega)|^2 \cdot S_x(\omega) \quad (26)$$

where

$S_y(\omega)$  is the power spectrum of the response process.

$S_x(\omega)$  is the power spectrum of the input loading process.

$H(\omega)$  is the frequency response function.

The computer programs to obtain the equivalent linear damping coefficient and the spectra of the response quantities, displacement, strain and stress along the mooring line are presented in Appendix E.

The assumption that the sea state is a stationary, Gaussian process with zero mean ensures that the response processes are also stationary and Gaussian with zero mean. The variances of the response processes  $y$ ,  $\frac{dy}{dt}$  and  $\frac{d^2y}{dt^2}$  are<sup>(10)</sup>

$$\sigma_y^2 = \int_0^\infty S_y(\omega) d\omega$$

$$\sigma_{\dot{y}}^2 = \int_0^\infty \omega^2 S_y(\omega) d\omega$$

$$\sigma_{\ddot{y}}^2 = \int_0^\infty \omega^4 S_y(\omega) d\omega$$

and the average frequency of the response process,  $f_e$ , is<sup>(10)</sup>

$$f_e = \frac{1}{2\pi} \frac{\sigma_{\dot{y}}}{\sigma_y} \quad (27)$$

The distribution of the peak values,  $y_p$ , has been shown<sup>(11)</sup> to be

$$p_{\eta}(\eta) = \frac{1}{\sqrt{2\pi}} \left[ \epsilon e^{-\frac{\eta^2}{2\epsilon^2}} + (1-\epsilon^2)^{\frac{1}{\epsilon}} e^{-\frac{\eta^2}{2}} \int_{-\infty}^{\eta} \frac{(1-\epsilon^2)^{\frac{1}{2}}}{\epsilon} e^{-\frac{x^2}{2}} dx \right] \quad (28)$$

where

$$\eta = y_p / \sigma_y$$

$$\epsilon^2 = \frac{\sigma_y^2 \sigma_{\dot{y}}^2 - \sigma_{y\dot{y}}^2}{\sigma_y^2 \sigma_{\dot{y}}^2}$$

$y_p$  is the peak value of  $y$

$\epsilon$  is a bandwidth indicator. The density curve  $p_{\eta}(\eta)$  is shown in Fig. 4 for several values of  $\epsilon$ .

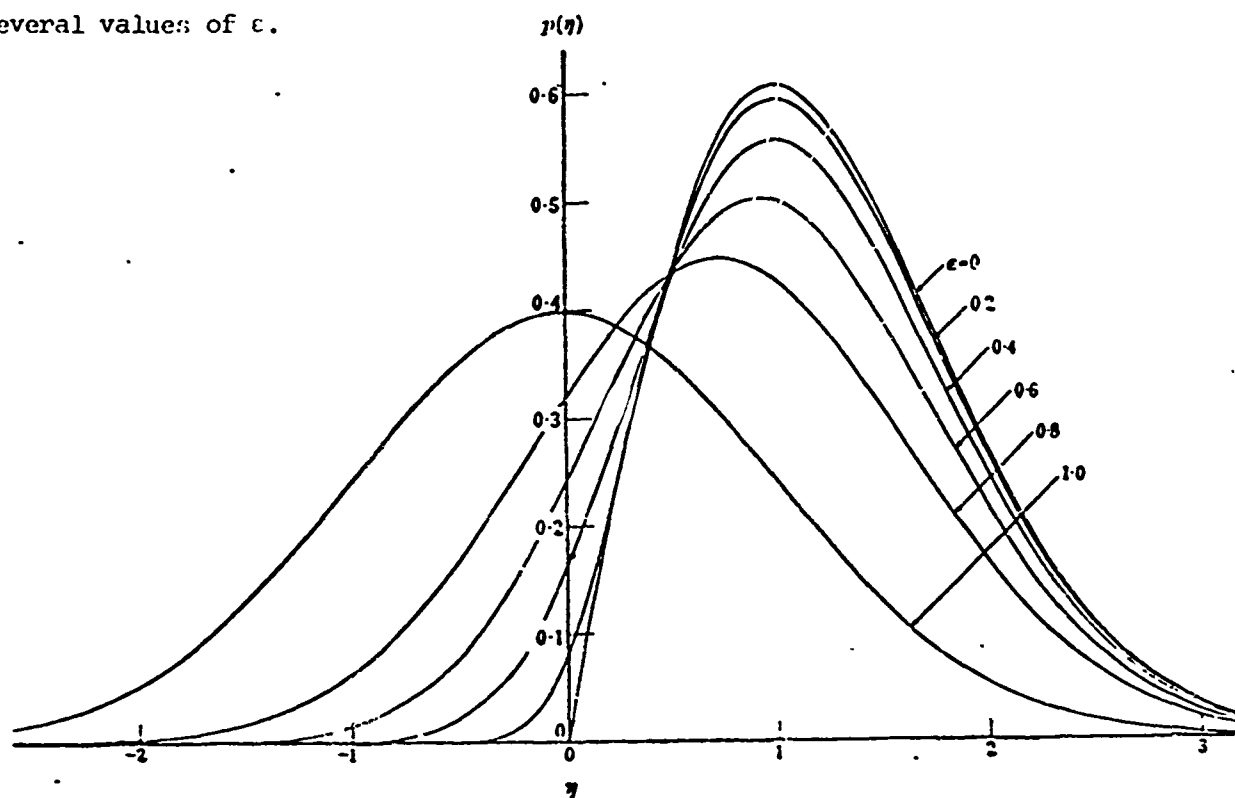


Fig. 4 Graphs of  $p_{\eta}(\eta)$ , the probability distribution of the heights of maxima ( $\eta = y_p / \sigma_y$ ) for different values of the width  $\epsilon$  of the energy spectrum. (11)

$p_{\eta}(\eta)$  is a Rayleigh curve when  $\epsilon = 0$ , whereas it is a Gaussian curve when  $\epsilon = 1$ . It is seen that the Rayleigh curve provides an upper bound distribution of the peak values. However, we are not interested in all peak values, but the maximum peak in two adjacent zero crossings. The distribution of the maximum peak values is shown to approximate the Rayleigh distribution as follows.

A zero-mean, Gaussian, stationary random signal is shown in Fig. 5.

Since we are interested in only the maximum value between two adjacent zero crossings (peak A), the peak B and peak C have to be excluded from Equation (28). The distribution after

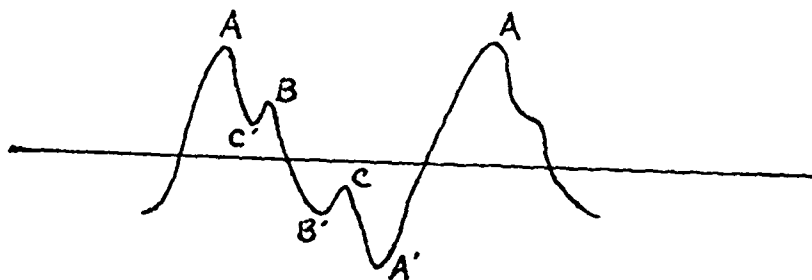


Figure 5. A zero-mean, Gaussian, stationary random signal.

excluding peak C is:

$$p_{AB}(\eta) = \frac{p_{\eta}(\eta)}{1 - \int_{-\infty}^0 p_{\eta}(\eta) d\eta} ; \eta \geq 0 \quad (29)$$

Considering:

- (1) The random process is symmetrical about zero mean, the probability of occurrence of peak C is the same as that of C'.
- (2) A peak C' accompanies a peak B.
- (3)  $\eta_B \geq \eta_{C'}$

The distribution of peak A may be approximated by excluding peak C and

peak C', instead of peak B, and conservative distribution thus obtained.

$$P_A(\eta) = \frac{1}{1-2 \int_{-\infty}^0 p_{\eta}(\eta) d\eta} [p_{\eta}(\eta) - p_{\eta}(-\eta)]; \eta \geq 0 \quad (30)$$

Substituting (28) into (30):

$$\begin{aligned} P_A(\eta) &= \frac{(1-\epsilon^2)^{\frac{1}{2}} \eta e^{-\eta^2/2}}{\sqrt{2\pi} (1-2 \int_{-\infty}^0 p_{\eta}(\eta) d\eta)} \left[ \int_{-\infty}^{\eta} \frac{(1-\epsilon^2)^{\frac{1}{2}}}{\epsilon} e^{-\frac{x^2}{2}} dx + \int_{-\infty}^{-\eta} \frac{(1-\epsilon^2)^{\frac{1}{2}}}{\epsilon} e^{-\frac{x^2}{2}} dx \right] \\ &= \frac{(1-\epsilon^2)^{\frac{1}{2}} \eta e^{-\eta^2/2}}{\sqrt{2\pi} (1-2 \int_{-\infty}^0 p_{\eta}(\eta) d\eta)} \left[ 2 \int_{-\infty}^0 e^{-\frac{x^2}{2}} dx + \int_0^{\eta} \frac{(1-\epsilon^2)^{\frac{1}{2}}}{\epsilon} e^{-\frac{x^2}{2}} dx + \int_0^{-\eta} \frac{(1-\epsilon^2)^{\frac{1}{2}}}{\epsilon} e^{-\frac{x^2}{2}} dx \right] \\ &= \frac{(1-\epsilon^2)^{\frac{1}{2}}}{1-2 \int_{-\infty}^0 p_{\eta}(\eta) d\eta} \eta e^{-\frac{\eta^2}{2}} \end{aligned}$$

since  $\int_0^{\infty} p_A(\eta) d\eta = 1$  and  $\int_0^{\infty} \eta e^{-\frac{\eta^2}{2}} d\eta = 1$

$$\therefore (1-\epsilon^2)^{\frac{1}{2}} = 1-2 \int_{-\infty}^0 p_{\eta}(\eta) d\eta$$

This coincides with the solution derived by Cartright and Longuet-Higgins<sup>(11)</sup> from a different approach.

Then

$$P_A(\eta) = \eta e^{-\frac{\eta^2}{2}} \quad (31)$$

Equation (31) represents the normalized distribution curve after excluding the shaded area in Fig. 6.

From the above, it is seen that the distribution of the maximum peak values approximates the Rayleigh distribution and is on the safe side for all values of  $\epsilon$ . Therefore, the Rayleigh distribution will be used to represent the peak stress distribution for all values of  $\epsilon$  in the safety analysis.



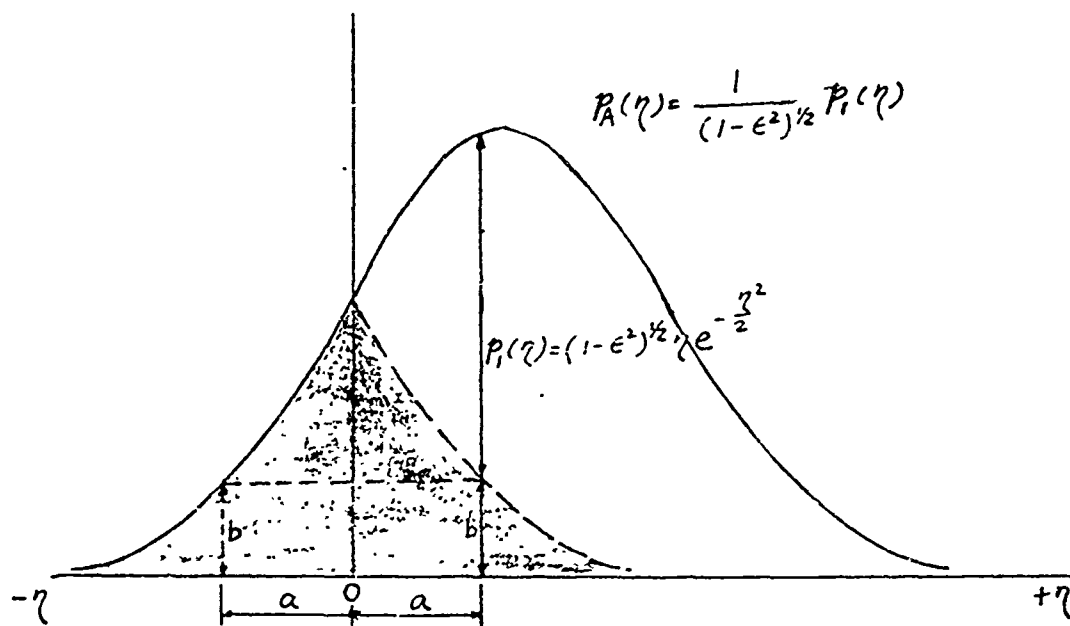


Figure 6. Density Curve of the Maximum Peak Values

## CHAPTER 4. DESIGN CONSIDERATIONS

The results of the previous work suggest the following critical design features.

### 4.1 Damping Parameters

The damping sources of a taut mooring line consist of the internal damping, the tangential drag on the rope surface, and the drag on the instrument package. The relative significance of the damping sources are shown in Figs. 7 and 8. The tangential drag on the rope surface is clearly a major damping source. The frequency response function is heavily dependent on the magnitude of the tangential drag coefficient as shown in Fig. 9. Evidently, a reliable estimate of the tangential drag coefficient is essential for an accurate assessment of the dynamic force in the mooring line. Such reliable data is not presently available.

The selection of a mooring rope should reflect the realization that different values of tangential drag coefficients will result in different dynamic behavior. The use of a rope with a very smooth surface may introduce a high resonant peak.

### 4.2 Dynamic Force Attenuation Along the Mooring Line.

The changes of the variance of the dynamic force along the mooring line are shown in Fig. 10, and the changes in the frequency response functions are displayed in Figs. 11, 12, and 13. It is evident that the higher the damping, the greater the attenuation of the dynamic force along the mooring line. For moderate or high damping, the maximum dynamic force is at the buoy; for low damping, the maximum force can be at depth.

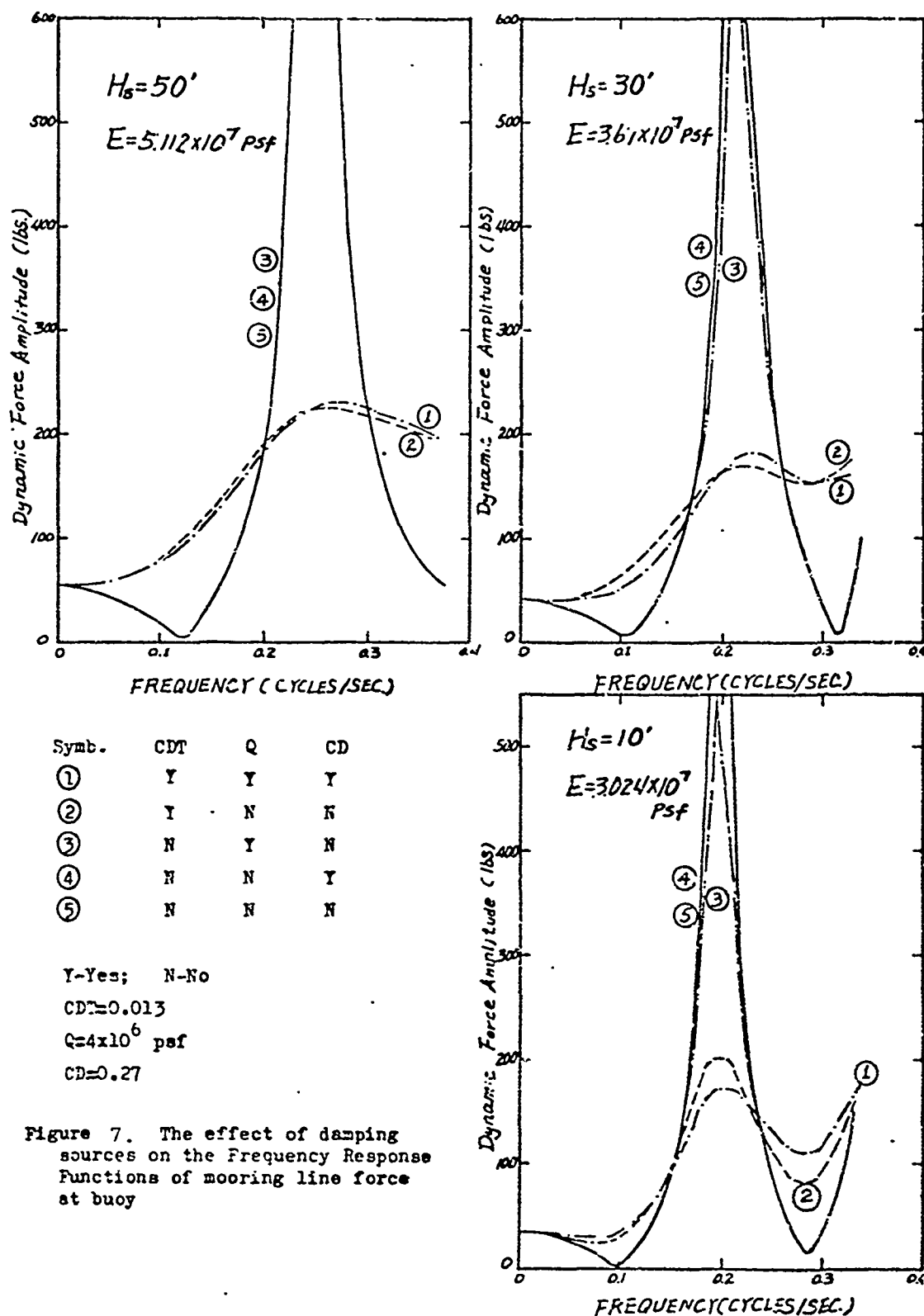
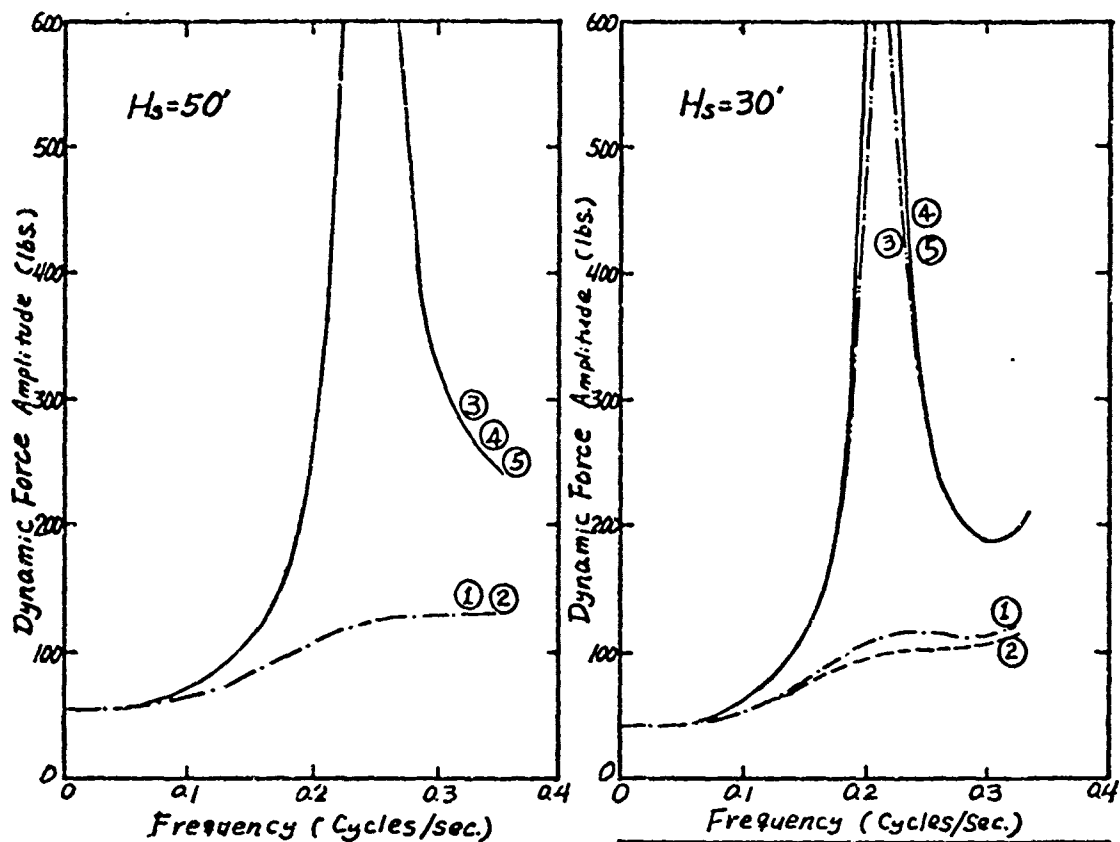


Figure 7. The effect of damping sources on the Frequency Response Functions of mooring line force at buoy



Symb.	CDT	Q	CD
①	Y	Y	Y
②	Y	N	N
③	N	Y	N
④	N	N	Y
⑤	N	N	N

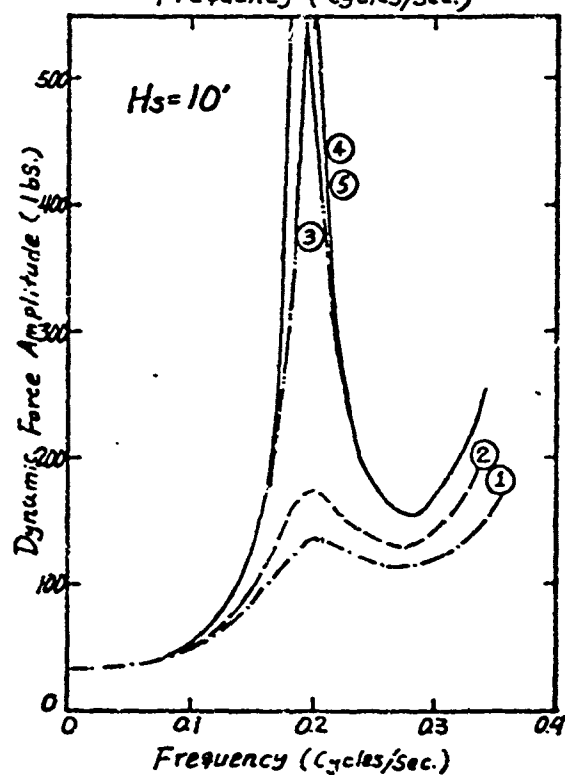
Y-Yes; N-No

CDT=0.015

$Q=4 \times 10^6$  psf

CD=0.27

Figure 8. The effect of damping sources on the Frequency Response Functions of the mooring line force at anchor



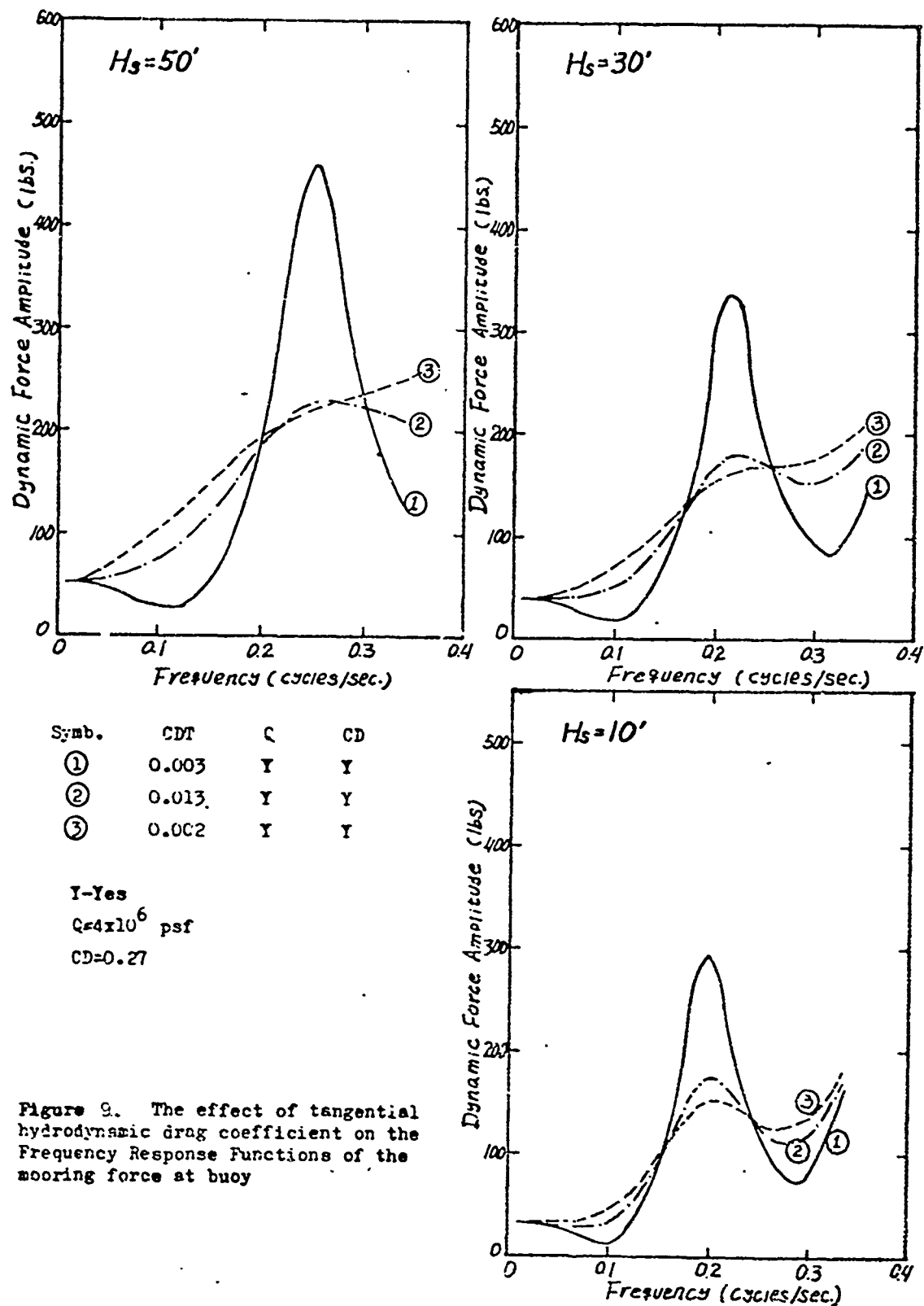


Figure 9. The effect of tangential hydrodynamic drag coefficient on the Frequency Response Functions of the mooring force at buoy

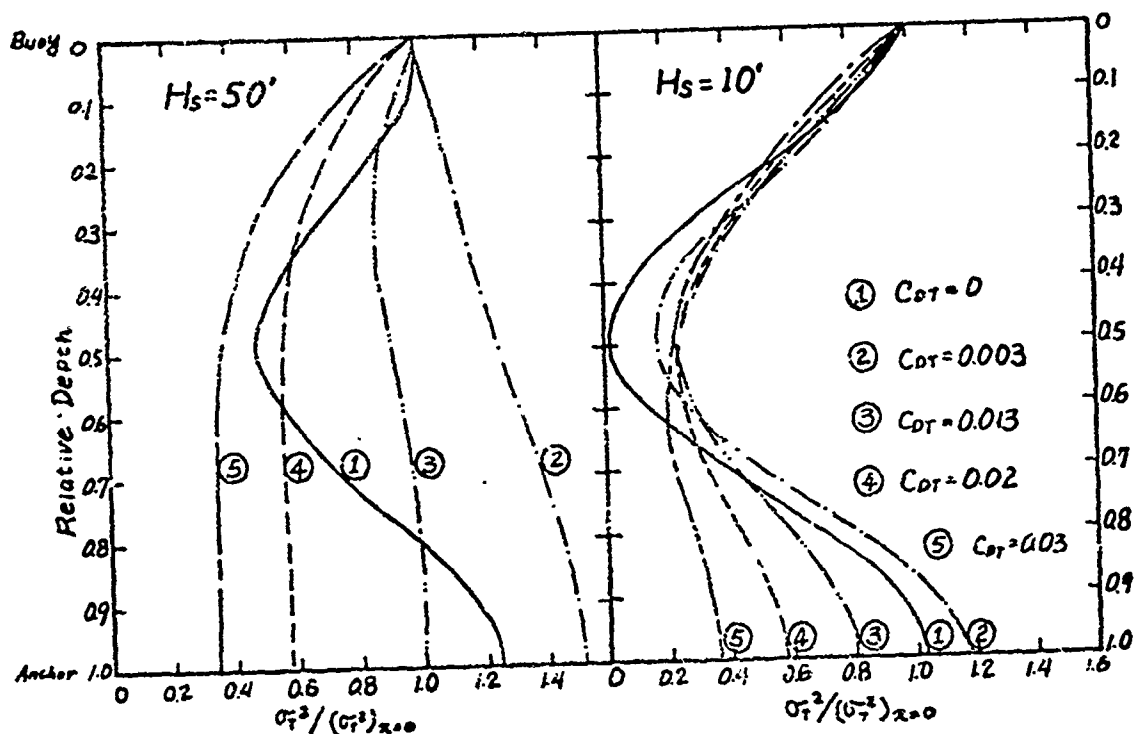


Figure 10. Variation of the Variance of the Dynamic force along the Mooring Line

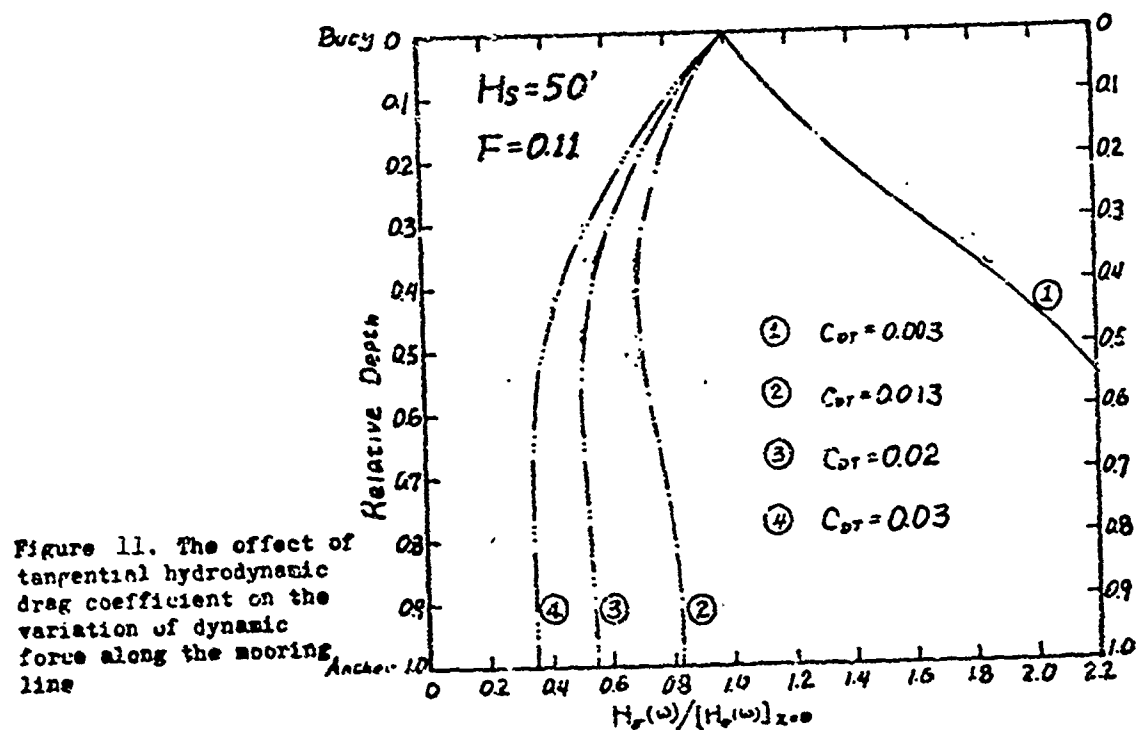


Figure 11. The effect of tangential hydrodynamic drag coefficient on the variation of dynamic force along the mooring line

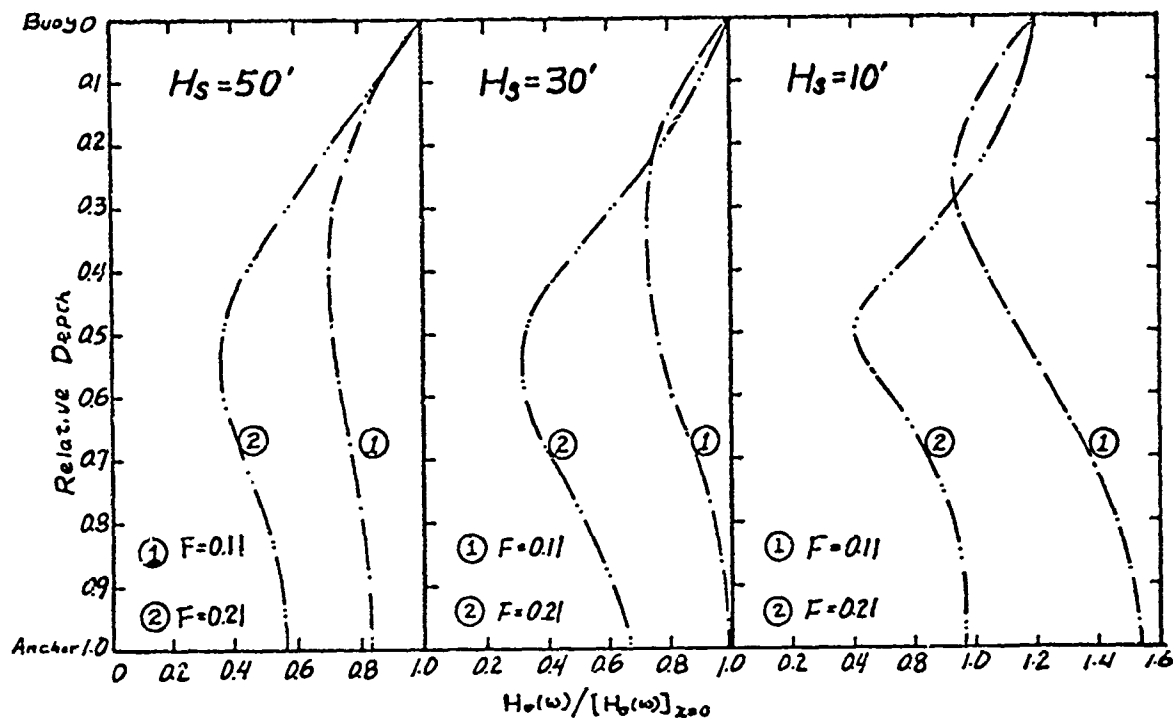


Figure 12. The effect of frequency on the dynamic force along the mooring line

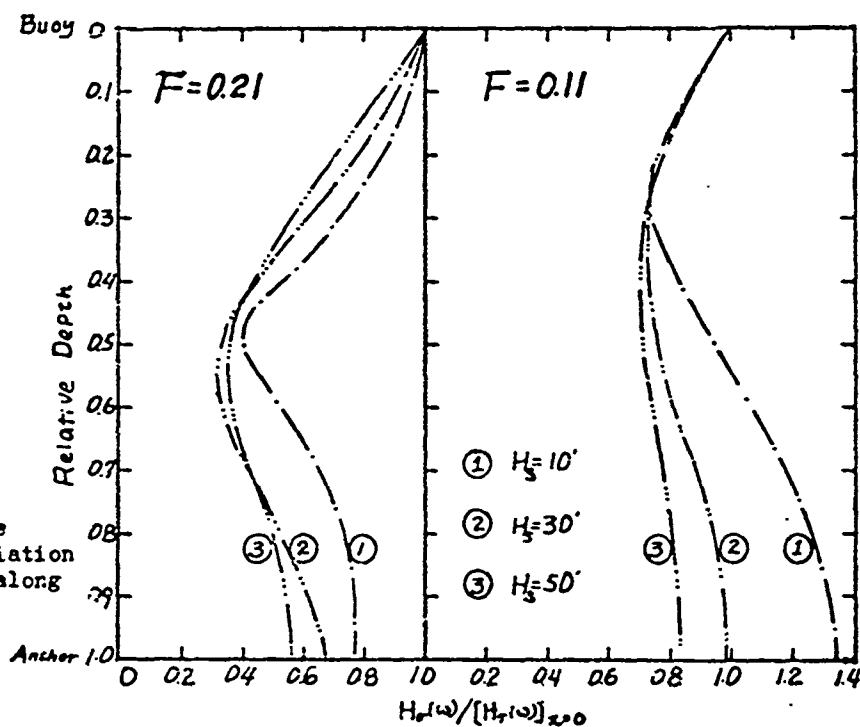


Figure 13.  
The effect of wave height on the variation of dynamic force along the mooring line

#### 4.3 Anchor Lifting

The mooring line force at the anchor results from three sources: configuration, wind and current drag, and wave excitation. The chance of anchor lifting can be minimized by adjusting the nylon scope and the rope combination (if a compound line is used) so that the dynamic force at the anchor is a minimum. Another alternative is to insert special dampers on the mooring line to cause attenuation of the dynamic motion for some distance from the anchor. The damper should be designed so that the drag coefficient is large in the axial direction and small in the lateral direction.



## CHAPTER 5. SUMMARY AND CONCLUSIONS

Computer programs for the steady state mooring line tension due to geometry, gravity, average current and average wind, and for the dynamic mooring line tension under the action of sine wave or random waves are presented in this report. The dynamic program is a frequency domain solution based on a linearized structural system and is only applicable to a taut line mooring. Specific points in this report are now summarized.

### Analytical Features

The non-linearity of a mooring line originates from three sources: hydrodynamic drag, line curvatures, and material properties. Solutions obtained in the time domain by using a simulated wave to generate the output history from either an analog or a digital computer are most satisfactory for mooring line dynamics. The high cost and special knowledge required in this method may not make it readily available for general design use. Alternatively, the dynamic response of a buoy system under random input can be obtained with a small amount of computer time from solutions in the frequency domain based on a linearized structural system. This method is developed here. The linearized structural system has the following features:

- (1) The line curvature non-linearity is neglected by treating the mooring line as a straight string.
- (2) The mooring rope is assumed to be made of step-wise linear, viscous material, and the loss modulus is taken to be always constant.
- (3) The hydrodynamic drag is linearized through the principle of equivalent linearization.

For a taut mooring line, the first and the second assumptions introduce negligible error; the third may bias the solution significantly in a high sea state. No error bound is available, and the solution can only be verified from experimental data.

### Forcing Conditions

The buoy is assumed to follow the sea surface, and the sea state is assumed to be a stationary, ergodic, Gaussian process with zero mean. Either a fully developed sea or an average sea spectrum is used as the loading spectrum in the analysis input.

Based on the linearized structural system, the dynamic force can be considered as a stationary Gaussian random process with zero mean, and the variance of the process is then derived. The total mooring line force is obtained from the superposition of the steady state force due to current and wind and the dynamic force due to waves; the total force is represented by a density curve. The distribution of the peak transient force is shown to approximate the Rayleigh distribution.

### Damping

The damping force on a mooring line comes from three sources: internal damping, water drag on the rope surface, and water drag on the instrument package. For a typical mooring without sub-surface buoy or special dampers inserted on the line, the water drag on the rope surface has been shown to be predominant. The dynamic behavior of the mooring line is heavily dependent on the value of the tangential drag coefficient. Neither theoretical solutions nor experimental data are available for the estimation of the tangential drag coefficient of a rope under oscillating motion. This must be remedied if a better assessment of the dynamic behavior of a mooring line is to be obtained.

## APPENDIX A.

### HYDRODYNAMIC DRAG ON ROPE AND BUOY

#### A.1 Hydrodynamic Drag on the Mooring Rope

##### A.1.1 Steady State Flow

The drag force per unit length,  $F_{DN}$ , exerted by a fluid of mass density  $\rho$ , flowing with uniform velocity  $V$  in a normally transverse direction to an immersed circular cylinder of diameter  $D$ , can be expressed as

$$F_{DN} = \frac{1}{2} C_{DN} \rho D V^2 \quad (A.1)$$

The dimensionless parameter  $C_{DN}$  is largely independent of Reynold's Number,  $R$ , in the range  $100 \leq R \leq 5 \times 10^5$  as shown in Fig. A.1. A mooring line has  $2 \times 10^3 < R < 2 \times 10^5$ ,<sup>(13)</sup> for which  $C_{DN} \approx 1.2$  for a long, smooth cylinder. Surface roughness and strumming may raise this figure to 1.8. In mooring line design, a value between 1.2 and 1.8 is used;<sup>(2)</sup> for this work,  $C_{DN}$  is taken as 1.5. In the case where the fluid approaches the mooring line with an incidence angle, the normal component of the drag force may be calculated by<sup>(12)</sup>

$$F_{DN} = \frac{1}{2} C_{DN} \rho D V_n^2 = \frac{1}{2} C_{DN} \rho D V^2 \sin^2 \phi \quad (A.2)$$

$$F_{DT} = \frac{1}{2} C_{DT} \rho \pi D V_T^2 = \frac{1}{2} C_{DT} \rho \pi D V^2 \cos^2 \phi \quad (A.3)$$

where  $\phi$  is the angle between flow direction and the mooring line.

Little data is available concerning the longitudinal drag on the mooring line. Based on the towing tests on finite length stranded cables, Podes<sup>(12)</sup> suggested the tentative relation,

$$C_{DT} = 0.02 C_{DN}$$

It was made clear that "The coefficient of the tangential force has not been measured accurately, but the results with respect to the tangential



coefficient agree at least in a qualitative way with the result of other experiments."<sup>(12)</sup> This point is further emphasized when it is noted that incidental flows, instead of parallel, were used in most of the cases where the tangential drag coefficient was measured.

The lower curves of Fig.A.1 show the theoretical results of Reid's analysis<sup>(13)</sup> for  $C_{DN}$  together with some experimental data from towing tests on stranded cables. The roughness parameter  $\lambda$  is defined as ratio of the equivalent sand-grain diameter of the surface roughness to the radius of the cylinder.

#### A.1.2 Tangential Drag Coefficient Under Sinusoidal Motion

The tangential hydrodynamic drag, which is considered to be negligible for the steady state mooring line analysis, may be a major factor in the response of a deep sea mooring line subject to oscillatory longitudinal motion at an end. This response is critical in the design of the structural system and therefore the tangential drag must be studied carefully.

The laminar boundary flow around a smooth circular cylinder under longitudinal sinusoidal motion may be obtained from the Navier-Stokes' equation<sup>(14)</sup>

$$\frac{\partial^2 V}{\partial r^2} + \frac{1}{r} \frac{\partial V}{\partial r} = \frac{\rho}{\mu} \cdot \frac{\partial V}{\partial t}; \quad r \geq \frac{d}{2} \quad (A.4)$$

and the time dependent boundary conditions

$$V = V_0 \cos \omega t \quad \text{at } r = d/2 \text{ for } t > 0$$

$$\text{and } V = 0 \quad \text{at } t = 0 \quad (A.5)$$

(A.4) and (A.5) correspond to the heat conduction equation in a circular cylinder with sinusoidal boundary conditions. The solution of the above equations are<sup>(15)</sup>

$$\frac{V}{V_0} = A \cos \omega t + B \sin \omega t + C$$

where A, B and C are functionals of Bessel functions. The detailed representation

of A, B and C can be found in Carslaw and Jaeger.<sup>(15)</sup> The tangential drag force per unit length then may be evaluated from

$$\begin{aligned} F_{DT} &= \pi d \tau = \pi d \rho \nu \left( \frac{\partial V}{\partial r} \right)_{r=d/2} \\ &= \pi d \rho \nu V_0 \left[ \frac{\partial A}{\partial r} \cos \omega t + \frac{\partial B}{\partial r} \sin \omega t + \frac{\partial C}{\partial r} \right]_{r=d/2} \end{aligned} \quad (A.6)$$

where  $\nu$  is the dynamic viscous coefficient. Rather than complete this numerical evaluation, an order of magnitude is obtained by determining the drag force on an infinite plate under sinusoidal motion. The solution of the laminar boundary flow of an infinite plate under sinusoidal motion is<sup>(14)</sup>

$$V(x, t) = V_0 e^{-\sqrt{\frac{\omega}{2\nu}} x} \cos(\omega t - \sqrt{\frac{\omega}{2\nu}} x) \quad (A.7)$$

where  $x$  is the distance perpendicular to the plate

$V_0$  is the velocity amplitude.

Then

$$\begin{aligned} \left( \frac{\partial V}{\partial x} \right)_{x=0} &= V_0 \sqrt{\frac{\omega}{2\nu}} (\sin \omega t - \cos \omega t) \\ &= V_0 \sqrt{\frac{\omega}{\nu}} \sin \left( \omega t - \frac{\pi}{4} \right) \end{aligned} \quad (A.8)$$

Substituting  $\rho = 1.935 \text{ lb. sec}^2/\text{ft}^4$ ,  $\nu = 10.9 \times 10^{-6} \text{ ft}^2/\text{sec}$  for water at 20°C., the tangential drag force due to skin friction is

$$\begin{aligned} F_{DT} &= \pi d \rho \nu V_0 \sqrt{\frac{\omega}{\nu}} \sin \left( \omega t - \frac{\pi}{4} \right) \\ &= 3.30 \times 10^{-3} \rho \pi d V_0 \sqrt{\omega} \sin \left( \omega t - \frac{\pi}{4} \right) \end{aligned} \quad (A.9)$$

From (A.6) and (A.9) it may be concluded that for smooth cylinder at laminar flow condition, the tangential drag coefficient is of the order of  $10^{-3}$  and is not proportional to  $V^2$  but  $V\sqrt{\omega}$  with a phase difference.

Surface roughness results in form drag rather than skin friction,<sup>(14)</sup> and the drag may be considered as proportional to the square of the velocity. For the drag of an oscillatory tangential flow on a rough surface, no theory and

experimental data are available.

It is suggested that the theoretical solution by Reid for the case of steady flow be used as a guide to assess the drag coefficient. Values for the roughness parameter  $\lambda$  are taken as 1.0, 0.2 and 0.01; the associated tangential drag coefficients, from Fig. A.1, are 0.013, 0.008 and 0.0035 for plaited rope, braided rope, and Nolaro respectively. These values are thought to reflect the relative roughness of these ropes.

## A.2 Wind and Current Drag on the Surface Buoy

### A.2.1 Physical Description of the Large Discuss Buoy

The large discuss buoy which was developed by General Dynamics will be used for this study on the merits of its surface following property. The buoy<sup>(8)</sup> is 40 feet in diameter and 7 feet thick with a flat deck and truncated cone shaped underside. The weight of the buoy, including the ballast, is about  $2 \times 10^5$  pounds and the moment of inertia about the horizontal axis through the center of gravity is  $7.5 \times 10^5$  slug-ft<sup>2</sup>.

The dimensions of the buoy are shown in Figs. A.2 and A.3.

### A.2.2 Buoy Wind Drag

Based on the results of wind tunnel tests on a scale model, Nath<sup>(16, 6)</sup> suggested the wind drag force on a 40 foot diameter discuss buoy as

$$F_w = 140 \rho_{air} \frac{W_a^2}{2} = 70 \rho_{air} W_a^2 \text{ (lbs)} \quad (A.10)$$

Introducing  $\rho_{air} = 0.00228$  slug/ft<sup>3</sup>.

$$\text{Then } F_w = 0.16 W_a^2 \text{ (lbs)} \quad (A.11)$$

where  $W_a$  is the ambient wind velocity in ft/sec.

The wind velocity increases with height above the sea. For a conservative picture the speed at the mast top (elevation 44') will be used in this analysis.

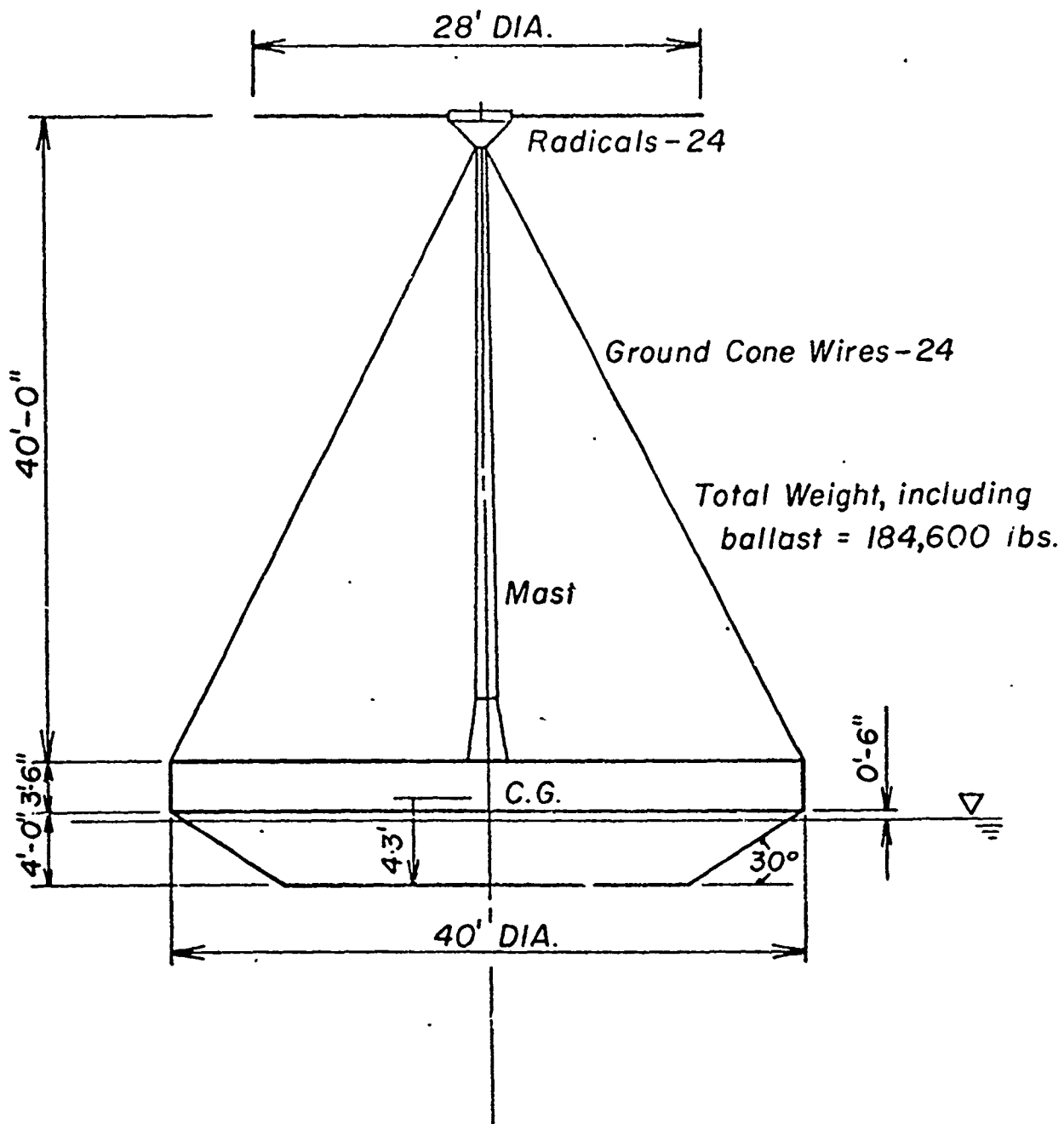
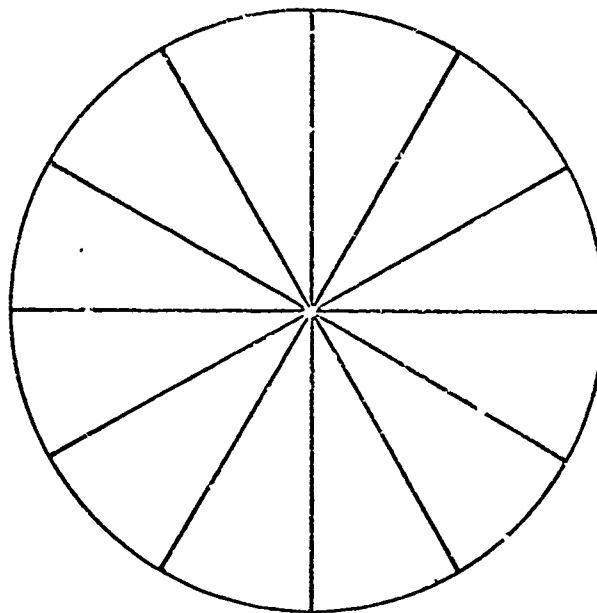


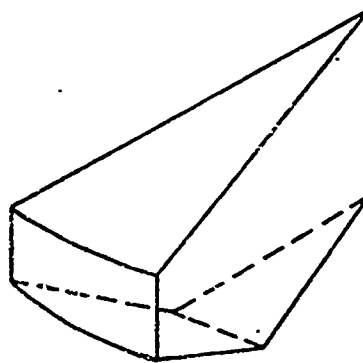
Figure A.2 Dimension of the discus buoy used in this study





*Note: The buoy was  
divided into 12 pieces  
for the initial work*

*a) Plan*



*b) Perspective of one segment*

Figure A.3      Detail of the buoy hull

Using the wind profile suggested by Davenport<sup>(17)</sup>

$$\frac{W_1}{W_2} = \left(\frac{Z_1}{Z_2}\right)^{1/\alpha} \quad (\text{A.12})$$

where  $\alpha = 8.5$  and  $30' \leq Z \leq 800'$  for winds over the water,

$$\text{then } (W)_{Z=44'} = \left(\frac{44}{64}\right)^{1/8.5} (W)_{Z=64'} = 0.957 (W)_{Z=64'}$$

It is to be mentioned that for very stormy conditions the air contains spray, which will increase the mass density and decrease the wind speed. The spray can be considered to be the result of energy transfer from wind to the ocean surface, and the total momentum flux of the wind layer near the sea level may be reduced due to the energy dissipation in the spray generation. Therefore, the use of a uniform wind velocity based on the magnitude at the top of the structure may result in a safe design for the wind force, including the effect of the spray. However, little is known about the true effect of the spray.

#### A.2.3 Buoy Hydrodynamic Drag

Hydrodynamic characteristics of various buoy hulls can be found in Hoerner,<sup>(18)</sup> Paquette and Henderson,<sup>(2)</sup> and Mercier.<sup>(19)</sup> The horizontal current drag on the large discus buoy was suggested by Nath<sup>(6)</sup> to be

$$\begin{aligned} F_{DC} &= 0.035 \times \frac{\pi}{4} (40)^2 \frac{V_c^2}{2} \rho_w \\ &= 22 \rho_w V_c^2 = 44 V_c^2 \text{ (lbs)} \end{aligned}$$

where  $V_c$  is the surface current velocity in ft/sec.

## APPENDIX B.

### DISCUSSION OF THE MODEL SIMPLIFICATIONS

#### B.1 Surface Following Property

Under wave excitation, the forces acting on a free floating buoy are buoyancy, initial force, and hydrodynamic damping. If the increment of buoyant force is much bigger than the increment of initial force under water undulation, the buoy will follow the water surface closely, and the surface follower buoy is named as a result of this phenomenon. The huge discus buoy is a typical example of this type. On the other extreme, if the increment of buoyant force is much smaller than the increment of initial force, then the buoy will not be disturbed significantly by the wave and will thus remain stationary. The spar buoy is a typical example of the stationary type. Other types of buoys fall between these two extremes.

The wave spectrum measured from a free floating wave meter (FFWM) when compared to that from a slack moored large discus buoy by Gaul and Brown,<sup>(20)</sup> indicates that the discus buoy behaves much as the FFWM at frequencies up to  $\frac{1}{4}$  Hz.

Comparison of these spectra is shown in Fig. B.1. The increment of mooring line tension may restrain the buoy motion and hence distort the response spectrum. However, the increment of mooring line tension is usually small compared to the increment of buoyant force for the discus buoy.

Fig. B.1 supports the assumption that the buoy response spectrum can be considered the same as the wave spectrum for design purposes.

It is suggested that wave spectrum be truncated at a frequency of 0.35 for the large discus buoy. For smaller surface follower buoys, the effective frequency range may be extended.

The computer program developed for the dynamic analysis of the mooring

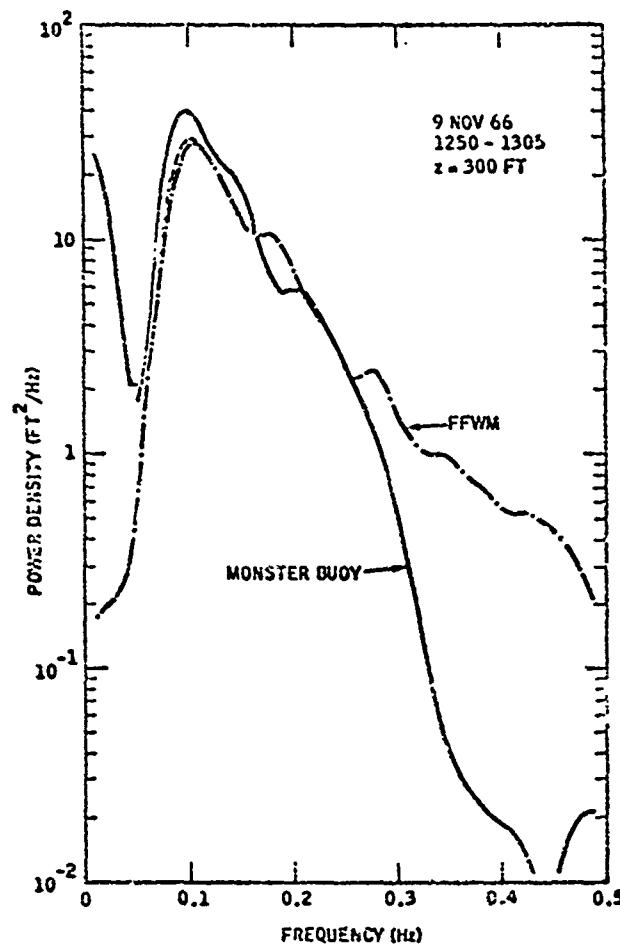


Figure B.1 Comparative Wave Spectra from FFWM and Monster Buoy.

line is based on the assumption that the buoy is a perfect surface follower. For buoys other than this type, a transfer function between the wave spectrum and the buoy response spectrum has to be established before a good result may be expected. However, the assumption will provide an upper bound solution to the dynamic stress of the mooring line provided the natural frequency of the heave motion of the buoy is far from the effective wave frequency. In the case of a stationary buoy, the dynamic force may be considered to be negligible.

## B.2 Straight String and Horizontal Buoy Motion

The mooring line does not remain straight under the action of ocean current. The sag will depend on the magnitude of mooring line tension and the current velocity. The effect of lateral loads on the dynamic force of a vibrating stretched string is investigated here.

Consider a stretched string with normal lateral loading  $q(x)$  as shown in Fig. B.2.

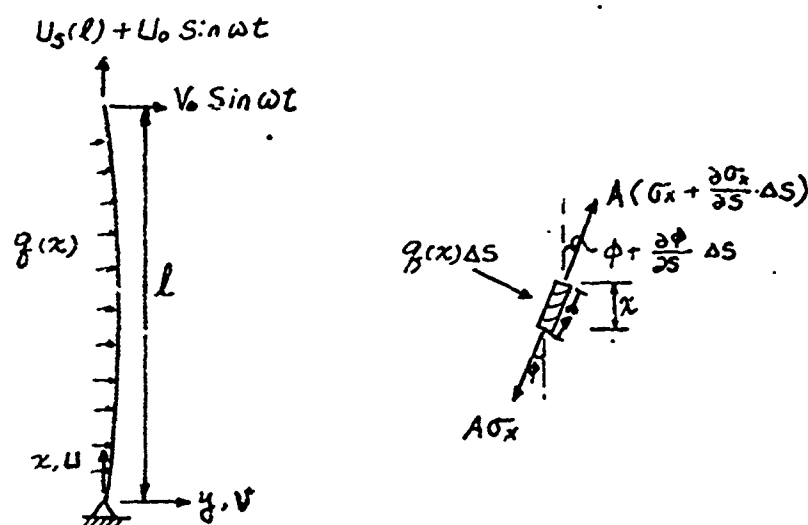


Figure B.2 Vibrating Stretched String Under Lateral Loading.

From equilibrium consideration in the  $x$  and  $y$  directions,

$$A\sigma_x \cos\phi - A\left(\sigma_x + \frac{\partial\sigma_x}{\partial S} \Delta S\right) \cos\left(\phi + \frac{\partial\phi}{\partial S} \Delta S\right) + m\Delta S \ddot{U} + q(x)\Delta S \sin\phi = 0 \quad (\text{B.1})$$

and

$$A\sigma_x \sin\phi - A\left(\sigma_x + \frac{\partial\sigma_x}{\partial S} \Delta S\right) \sin\left(\phi + \frac{\partial\phi}{\partial S} \Delta S\right) - m\Delta S \ddot{V} - q(x)\Delta S \cos\phi = 0 \quad (\text{B.2})$$

For a prestretched string, the longitudinal displacement  $U$  can be divided into a static component,  $U_s(x) = \epsilon_s x$  and a dynamic component,  $U_D(x, t)$ ,

$$U(x, t) = U_s(x) + U_D(x, t)$$

where  $\epsilon_s$  is the prestretched strain.

For a deep sea, taut mooring line:

$$l \gg U_S(l) \gg U_D$$

$$V_0 \approx U_0/4 \quad (31)$$

$\epsilon_S$  is of the order of 0.1.

$\frac{\partial U_D}{\partial x}$  and  $\frac{\partial V}{\partial x}$  are usually of the same order and much smaller than  $\epsilon_S$  except at resonance frequencies. However, a resonance condition is not likely to be developed due to the internal and external dampings. Based on these, the following approximations are made:

$$\Delta S \approx \Delta X$$

$$\sin \phi \approx \phi$$

$$\cos \phi \approx 1$$

$$\epsilon = \frac{\partial U}{\partial X} + \frac{1}{2} \left( \frac{\partial V}{\partial x} \right)^2 \approx \frac{\partial U}{\partial x}; \quad \epsilon \text{ is the axial strain of the string.}$$

After neglecting the second order terms, Equation (B.1) and (B.2) may be rewritten as:

$$\frac{\partial^2 U_D}{\partial x^2} - \frac{1}{a^2} \frac{\partial^2 U_D}{\partial t^2} = \frac{q(x)}{AE} \frac{\partial V}{\partial x} \quad (B.3)$$

$$\frac{\partial^2 U_D}{\partial x^2} \frac{\partial V}{\partial x} + \frac{\partial U_D}{\partial x} \cdot \frac{\partial^2 V}{\partial x^2} - \frac{1}{a^2} \frac{\partial^2 V}{\partial t^2} = - \frac{q(x)}{AE} \quad (B.4)$$

where  $a^2 = E/\rho$ ;  $\rho$  is the mass density.

Equations (B.3) and (B.4) appear analytically intractable. In order to see the effect of the term  $\frac{q(x)}{AE} \frac{\partial V}{\partial x}$  on the solution of  $U_D$ , an approximate solution is presented.

The equations of longitudinal and transverse small amplitude vibrations of a stretched string without lateral loading as deduced from Equations (B.3) and (B.4) are

$$\frac{\partial^2 U_D}{\partial x^2} - \frac{1}{a^2} \frac{\partial^2 U_D}{\partial t^2} = 0 \quad (B.5)$$

$$\frac{\partial^2 V}{\partial x^2} - \frac{1}{b^2} \frac{\partial^2 V}{\partial t^2} = 0 \quad (B.6)$$

where  $b^2 = \frac{T}{m}$ ;  $m$  is the effective mass per unit length,

$T$  is the pretension in the string.

The solution of Equation (B.5) with boundary conditions:

$$U_D = 0 \quad \text{at } x = 0$$

$$U_D = U_0 \sin \omega t \quad \text{at } x = l$$

is 
$$U_D + \frac{U_0}{\sin \frac{\omega l}{a}} \sin \frac{\omega}{a} x \sin \omega t \quad (B.7)$$

The solution of Equation (B.6) with boundary conditions:

$$V = 0 \quad \text{at } x = 0$$

$$V = V_0 \sin \omega t \quad \text{at } x = l$$

is

$$V = \frac{V_0}{\sin \frac{\omega l}{b}} \sin \frac{\omega}{b} x \sin \omega t \quad (B.8)$$

Using (B.7) and (B.8), then

$$\frac{\partial^2 U_D}{\partial x^2} \cdot \frac{\partial V}{\partial x} = \frac{b}{a} \frac{\partial^2 V}{\partial x^2} \frac{\partial U_D}{\partial x} \quad (B.9)$$

where  $\frac{b}{a} = \sqrt{\frac{T}{AE}}$

Introducing (B.9), Equation (B.4) can be reduced to

$$\frac{\partial^2 y}{\partial x^2} - \frac{1}{(1 + \frac{b}{a})b^2} \frac{\partial^2 y}{\partial t^2} = - \frac{q(x)}{AE} \quad (B.10)$$

which has a solution

$$V(x,t) = \frac{V_0}{\sin \frac{\omega l}{B}} \sin \frac{\omega}{B} x \sin \omega t + \int \int \frac{q(x)}{AE} dx dx + D_1 x + D_2 \quad (B.11)$$

where  $B^2 = (1 + \frac{b}{a})b^2$ , and the constants  $D_1$  and  $D_2$  can be determined from

$$V = 0 \quad \text{at } x = 0, \quad t = 0$$

$$V = 0 \quad \text{at } x = l, \quad t = 0$$

Using Equation (B.11) in (B.3) gives

$$\frac{\partial^2 U_D}{\partial x^2} - \frac{1}{a^2} \frac{\partial^2 U_D}{\partial t^2} = \frac{q(x)}{AE} \left[ \frac{V_0 \frac{\omega}{B}}{\sin \frac{\omega l}{B}} \cos \frac{\omega x}{B} \sin \omega t - \int \frac{q(x)}{AE} dx + D_1 \right] \quad (B.12)$$

For a special case where  $q(x) = q_0 = \text{constant}$

$$D_1 = + \frac{q_0}{2AE}$$

$$D_2 = 0$$

and Equation (B.12) reduces to

$$\frac{\partial^2 U_D}{\partial x^2} - \frac{1}{a^2} \frac{\partial^2 U_D}{\partial t^2} = \frac{q_0}{AE} \left[ \frac{V_0 \frac{\omega}{B}}{\sin \frac{\omega l}{B}} \cos \frac{\omega x}{B} \sin \omega t - \frac{q_0 x}{AE} + \frac{q_0}{2AE} \right] \quad (B.13)$$

which has a solution

$$U_D = (C_1 \sin \frac{\lambda}{a} x + C_2 \cos \frac{\lambda}{a} x)(C_3 \sin \lambda t + C_4 \cos \lambda t) + \frac{q_0 V_0 \frac{\omega}{B}}{(\frac{\omega^2}{a^2} - \frac{\omega^2}{B^2})AE \sin \frac{\omega l}{B}} \cos \frac{\omega x}{B} \sin \omega t - \frac{q_0^2}{6A^2 E^2} x^3 + \frac{q_0 x^2}{4A^2 E} \quad (B.14)$$

The last two terms in (B.14) involve only spatial variables. They may add to the static component and be neglected in the dynamic analysis. With this in mind and letting

$$Q = - \frac{q_0 V_0 \frac{\omega}{B}}{(\frac{\omega^2}{B^2} - \frac{\omega^2}{a^2})AE \sin \frac{\omega l}{B}} \quad (B.15)$$



Then

$$U_D(x,t) = (C_1 \sin \frac{\lambda}{a} x + C_2 \cos \frac{\lambda}{a} x)(C_3 \sin \lambda t + C_4 \cos \lambda t) + Q \cos \frac{\omega}{B} x \sin \omega t \quad (B.16)$$

Introducing the boundary conditions,

$$(1) \quad U_D = 0 \quad \text{at } t = 0$$

$$(2) \quad U_D = 0 \quad \text{at } x = 0$$

$$(3) \quad U_D = U_D \sin \omega t \quad \text{at } x = l$$

Allow Equation (4.30) to be expressed by

$$U_D(x,t) = \left[ \frac{U_0}{\sin \frac{\omega}{a} l - Q(\cos \frac{\omega l}{a} - \cos \frac{\omega l}{B})} \sin \frac{\omega}{a} x - Q \cos \frac{\omega}{a} x + Q \cos \frac{\omega x}{B} \right] \sin \omega t \quad (B.17)$$

Comparison between Equations(B.7) and (B.17) indicates that the effect of lateral loading on the dynamic force of the string is negligible if  $Q \ll 1$ . On the examination of (B.16), it is seen that  $Q$  is usually less than unity by several orders except when  $\sin \frac{\omega l}{B} \rightarrow 0$ . This is the condition where the transverse resonance occurs, and the solution based on small amplitude vibration does not apply.

In the case of a deep sea mooring line, the interaction between water and rope will damp the transverse motion and the effect of the lateral loading may be considered to be small for all conditions.

### B.3 Damping Linearization

Based on the principle of equivalent linearization,<sup>(21)</sup> the solution of a non-linear equation

$$M \ddot{X} + K X + \mu f(X, \dot{X}) = 0 \quad (B.18)$$

may be approximated by the solution of an equivalent linear equation

$$M \ddot{X} + (K + K_1) X + \lambda \dot{X} = 0 \quad (B.19)$$

The equivalent parameters  $K_1$  and  $\lambda$  are obtained by equating the work per cycle for the two systems. The magnitude of the error depends on the linearized quantities  $(\frac{\lambda}{M})^2$  and  $(\frac{\lambda}{K})^2$  and is of the order of magnitude of  $\mu^2$ .<sup>(21)</sup> In general, if  $\mu f(X, \dot{X})$  is small compared to  $M \ddot{X}$  and  $K X$ , the error will be small. The parameter  $\lambda$  is obtained by equating the active components of energy in both systems,  $K_1$  by equating the reactive components. Assuming

$$X = a \cos (\omega t + \phi) \quad (B.20)$$

$\lambda$  and  $K_1$  have been shown<sup>(21)</sup> to be

$$\lambda = \frac{\mu}{\pi a \omega} \int_0^{2\pi} f(a \cos \phi, -a \omega \sin \phi) \sin \phi \, d\phi \quad (B.21)$$

$$K_1 = \frac{\mu}{\pi a} \int_0^{2\pi} f(a \cos \phi, -a \omega \sin \phi) \cos \phi \, d\phi \quad (B.22)$$

where  $\omega^2 = \frac{k}{M}$

The equivalent linearized damping coefficients of the hydrodynamic drag on the instrument package and the mooring line are derived as follows.

#### (A) Instrument Package

The hydrodynamic drag on the instrument package is

$$F_{DP} = \frac{1}{2} C_{DN} A \rho \omega |\dot{X}| \quad \dot{X} = \mu |\dot{X}| \quad \dot{X} = \lambda \dot{X}$$

where  $C_{DN}$  is the dimensionless normal drag constant

$A$  is the projected area of the package on the plane perpendicular to the motion.

From (B.21) and (B.22)

$$\lambda = \frac{1}{3\pi} \rho \omega C_{DN} A a \omega \quad (B.23)$$

$$K_1 = 0 \quad (B.24)$$

The magnitude of error will depend on the weight, volume, and geometry of the package. It will be smaller with a slender current meter compared to a glass ball. When the water drag on the packages are not the major system damping force, the linearization technique may be applied to all packages without excessive solution distortion. However, the arguments only provide a guide for subsequent employment of engineering judgment and the accuracy may only be checked by comparison with experimental results.

#### (B) Mooring Line

The hydrodynamic drag on the mooring line surface per unit length is given by  $F_{DR} = \frac{1}{2} C_{DT} A \rho_w |\dot{X}| \dot{X} = \mu |\dot{X}| \dot{X} \approx \lambda \dot{X}$  where

$C_{DT}$  is the tangential drag coefficient

$A = \pi D$  is the surface area per unit length.

From (B.21) and (B.22)

$$\lambda = \frac{4 \rho_w C_{DT} D \omega a}{3} \quad (B.25)$$

$$K_1 = 0 \quad (B.26)$$

Normally  $\lambda = \lambda(x)$ .

However to ensure an analytical solution to the linearized equation,  $\lambda$  has to be assumed constant for the whole section of the mooring line. This equivalent coefficient is obtained from the balance of energy dissipated in the whole section of the mooring line in one cycle; this results in the equation

$$\int_0^L \int_0^T (\lambda \dot{X}) \dot{X} dt dX = \int_0^L \int_0^T \left( \frac{C_{DT}}{2} \rho_w \pi D |\dot{X}| \dot{X} \right) dt dX$$

giving

$$\lambda = \frac{4 \rho_w C_{DT} D \omega}{3} \frac{\int_0^L a^3(x) dx}{\int_0^L a^2(x) dx} \quad (B.27)$$

The tangential drag is usually very small compared to the initial force and the elastic restoring force; because of this, the method of equivalent linearization usually achieves good results.

#### B.4 Internal Linear Damping of the Mooring Line

The areas of the hysteresis loops under cyclic axial tension of the nylon ropes have shown that the internal damping is not linear. When the internal damping is a major damping source, then the non-linear damping may be linearized by using a stress dependent loss modulus. The problem may then be solved by an iteration process. Usually the effect of the internal damping is relatively small compared to the hydrodynamic damping; therefore, only a rough estimate of the loss modulus is used in the solution program.

#### B.5 Strumming

Little is known about mooring line strumming and its effect. The purpose of the assumption of neglecting the effect of strumming is to simplify the problem so that it can be handled analytically. However, the effect of the small amplitude transverse motion has been shown to be negligible in the mooring line dynamics, and it may be expected that the strumming will stay in the small amplitude region because of the damping forces and the irregular profile of the ocean current.

## APPENDIX C.- Program STEADY

### C.1 Purpose

To solve the steady state mooring line tension under the action of wind and current.

### C.2 Program Logic

The Program starts with the estimation of the inclination angle of the top segment. Knowing this and the horizontal drag coefficients in the buoy and the mooring line, the force of the top segment can be calculated and the position of the end of the segment is determined given the stress-strain relationship of the mooring line. According to (1) and (2), the force increment  $\Delta T$  and the angle increment  $\Delta \phi$ , then the end position of the second segment can be determined. In the same manner, the forces and end positions of the successive segments are determined. If the vertical position of the anchor thus obtained does not fall close to the water depth within a pre-set tolerable limit, then the inclination angle of the first segment is revised and the calculation is repeated. The iteration process repeats until a satisfactory solution is achieved.

### C.3 Notation

#### (A) Input

NLK	Number of cases
K	Number of line sections
CDB	Current drag coefficient on the buoy; the drag force $= CDB \cdot V_c^2$ ; $V_c$ is current velocity.
CDW	Wind drag coefficient on the buoy; the drag force $= CDW \cdot V_w^2$ ; $V_w$ is wind velocity
CDT	Tangential hydrodynamic drag coefficient on the rope; the drag force $= \frac{1}{2} \rho_w \cdot CDT \cdot \pi \cdot D \cdot V_{CT}^2$ per unit length.

CDN Normal hydrodynamic drag coefficient on the rope; the  
drag force =  $\frac{1}{2} \rho_W \text{ CDN} \cdot D \cdot V_{CN}^2$  per unit length.

VC0 Surface velocity of the ocean current with zero wind  
velocity, in knots.

LP Length of the package, in feet.

WP Weight of the package, in pounds.

CDNP Normal hydrodynamic drag coefficient on the package; the  
drag force =  $\text{CDNP} V_{CN}^2$ ; lb.-sec<sup>2</sup>/ft.<sup>2</sup>

CDTP Tangential hydrodynamic drag coefficient on the package;  
the drag force =  $\text{CDTP} V_{CT}^2$ ; lb.-sec<sup>2</sup>/ft.<sup>2</sup>

SA Length in feet of the small increment of the rope considered  
to be straight. It must be a common factor to all line  
sections.

DEPTH Water depth in feet

ERR Tolerable error. The allowable difference between the water  
depth and the anchor depth is  $\text{ERR} \times \text{DEPTH}$ .

HS Significant wave height in feet.

UFA Average ultimate strength of the synthetic ropes in pounds.

L Length of the rope in feet

DIA Diameter of rope in inches

UF Ultimate strength of the rope in pounds.

UWT Weight of the rope in water in plf.

ZPERM Permanent strain of the rope at station (due to the anchor  
weight)

MC Material code: MC=0 for fiber rope, MC=1 for wire rope

NN Interval of the line increments for output printing.

(B) Output

X,Y Horizontal and vertical axis with the origin at the buoy  
in feet.

C.4 Remarks

(1) The stress-strain relationship used in this program is:

$$Z = 0.171 \text{ Exp}\left(-\frac{0.0819}{r}\right) + Z\text{PERM for the nylon line}$$

and  $Z = 0.0115r + Z\text{PERM}$  for the wire rope

where Z is the strain

r is the ratio of the force to the dry ultimate strength. The program should be modified for other stress-strain relationships.

(2) The convergence rate of the solution depends on the stress-strain relationship and the initial angle correction function. If the stress-strain relationship is changed, it is desirable to revise the correction function for a faster rate of convergence.

(3) The program capacity is limited to 20 line sections and 1000 increments. The core storage needed for this program is 40 K. The number of line sections and increments can be enlarged by changing the program dimensions.

(4) For a typical deep sea mooring with 300 line increments, it takes 3 or 4 seconds in CDC 6400 to obtain the results.

(5) Output information is self-explanatory.

C.5 Program Listing

```

PROGRAM STEADY (INPUT,OUTPUT,TAPE5=INPUT,TAPE6=OUTPUT)
DIMENSION PHI(1002),I(1001),X(1001),Y(1001),R(1001),Z(1001),MC(20)
1,L(20),UF(20),DIA(20),UWT(20),WP(20),MP(21),ST(1001),LP(20),CDNP(2
10),CDTP(20),ZPERM(20)
REAL L,LL,LP,LS
10 FORMAT (20I4)
11 FORMAT (5F8.0,14)
12 FORMAT ( 4F8.0)
13 FORMAT (4F6.0)
14 FORMAT (5F6.0)
15 FORMAT (2F8.0)
READ 10, NLK,K
PRINT 21, NLK,K
21 FORMAT ( *      NLK=*,I4,*      K=*,I4)
READ 14, CDB,CDW,CDT,CDN,VCO
PRINT 24, CDB,CDW,CDT,CDN,VCO
24 FORMAT ( *      CDB=*,E10.3,*      CDW=*,E10.3,*      CDT=*,E10.3,*
1 CDN=*,E10.3,*      VCO=*,E10.3)
READ 13, (LP(I),WP(I),CDNP(I),CDTP(I), I=1,N)
PRINT 23
23 FORMAT ( *      LP(I)      *,*WP(I)      *,*CDNP(I)      *,*CDTP(I)      *,*
1 I*)
PRINT 33, (LP(I),WP(I),CDNP(I),CDTP(I),I, I=1,N)
33 FORMAT (4F10.5,I10)
DO 2000 NL=1,NLK
READ 12, SA,DEPTH,ERR
PRINT 22, SA,DEPTH,ERR
22 FORMAT (1H1,*      SA=*,F0.2,*      DEPTH=*,F7.1,*      ERR=*,F6.0)
READ 15, HS,UFA
PRINT 25, HS,UFA
25 FORMAT ( *      HS=*,F4.1,*      UFA=*,F8.2)
READ 11, (L(I),DIA(I),UF(I),UWT(I),ZPERM(I),MC(I), I=1,N)
PRINT 28
28 FORMAT ( *      L(I)      *,*      DIA(I)      *,*      UF(I)      *,*      UWT
1(I)      *,*      ZPERM(I)      *,*      MC(I)      *,*      I*)
PRINT 38,(L(I),DIA(I),UF(I),UWT(I),ZPERM(I),MC(I),I, I=1,N)
38 FORMAT (5E14.3,2I10)
READ 10,NN
DO 45 I=1,K
LIA(I)=DIA(I)/12.
45 CONTINUE
MP(1)=1
DO 50 I=1,K
MP(I+1)=MP(I)+IFIX(L(I)/SA) +1
50 CONTINUE
C CALCULATE INITIAL ANGLE
LL=0.
DO 300 J=1,K
IF (MC(J).EQ.1) GO TO 300
LL=LL+L(J)*(1.+ZPERM(J))
300 CONTINUE
LS=0.
DO 310 J=1,K
IF (MC(J).EQ.0) GO TO 310
LS=LS+L(J)*(1.+ZPERM(J))
310 CONTINUE

```



```

      Z=LL+LS
      SCUPL=LL/(DEPT*PI*LS)
      ZA=(DEPT*PI)/LL
      ZZ=0.171777
      ZL=ALOG(ZZ)
      RA=0.0819/ZL
      FV=RA*UFA
C   ONI KNOL=1.68887 FPS
      IF (HS.GE.24.) GO TO 320
      VN=12.53*SQRT(HS)*0.957
      GO TO 336
326 VN=2.06*(HS+5.8)*0.957
336 VCS=(VCO+.023*VN)*1.68887
      HF=CDB*VA*ABS(VN)+CDB*VCS*ABS(VCS)
      R(1)=0.
      Z(1)=0.
      X(1)=0.
      Y(1)=0.
      JT(1)=0.
      F(1)=0.
      N=0
      PHI(1)=0.
      YDD=0.
      PHI(2)=ATAN(HF/FV)
      M2=1      ISTOP=1
100 FH=HF
C   PRINT 111, PHI(2),FH,YDD,Y(M2),ISTOP,M2
111 FORMAT (4E15.5,2I4)
      FV=FH/TAN(PHI(2))
      F(2)=SQRT(FH*FH+FV*FV)
      KD=0
      DO 1000 J=1,K
      M1=MP(J)+1
      M2=MP(J+1)-1
930 DO 935 I=M1,M2
      R(I)=F(I)/GF(J)
      RB=R(I)
      IF (MC(J).EQ.1) GO TO 950
C
C   STRESS-STRAIN RELATIONSHIP FOR NYLON ROPE
C
      Z(1)=0.171*EXP(-0.0819/RB)
      ZB=Z(1) +ZPERM(J)
      GO TO 955
C
C   STRESS-STRAIN RELATIONSHIP FOR WIRE ROPE
C
950 Z(1)=0.0115*R(1)      ZB=Z(1) +ZPERM(J)
955 SINP=SIN(PHI(1))
      COSP=COS(PHI(1))
      SB=SA*(1.+ZB)
      JT(I)=JT(I-1)+SB
      SBX=SB*SINP
      SBY=SB*COSP
      X(I)=X(I-1)+SBX
      Y(I)=Y(I-1)+SBY

```

```

C
C      CURRENT PROFILE
C
      YN=Y(I)-.5*SB*COSP
      YM=YN/3.28-10.
      IF (YM.GE.0.) GO TO 513
      VC=VCS
      GO TO 515
513 VC=VCJ/YM**0.4
515 VCN=VC*COSP
      VCT=VC*SINP
      D=DIA(J)/SQRT(1.+ZB)
      FCDN=SB*D*CDN*VCN*ABS(VCN)
      FCDT=SB*3.1416*D*CDT*VCT*ABS(VCT)
      F(I+1)=F(I)+FCDT-SA*UWT(J)*COSP
      FAV=(F(I)+F(I+1))/2.
      PHI(I+1)=PHI(I)+(FCDN+SA*UWT(J)*SINP)/FAV
935 CONTINUE
940 I=IP(J+1)
      R(I)=0.
      Z(I)=0.
      SINP=SIN(PHI(I))
      COSP=COS(PHI(I))
      X(I)=X(I-1)+LP(J)*SINP
      Y(I)=Y(I-1)+LP(J)*COSP
      Z(I)=Z(I-1)+LP(J)
      YN=Y(I)-.5*SB*COSP
      YM=YN/3.28-10.
      IF (YM.GE.0.) GO TO 613
      VC=VCS
      GO TO 615
613 VC=VCJ/YM**0.4
615 VCN=VC*COSP
      VCT=VC*SINP
      FCDN=CDNP(J)*VCN*ABS(VCN)
      FCDT=CDTP(J)*VCT*ABS(VCT)
      F(I+1)=F(I)+FCDT-WP(J)*COSP
      FAV=(F(I)+F(I+1))/2.
      PHI(I+1)=PHI(I)+(FCDN+WP(J)*SINP)/FAV
1000 CONTINUE
      N=N+1
C
C      INITIAL ANGLE CORRECTION
C
      YD=Y(M2)-DEPTH
      YDD=YD/DEPTH
      YDA=ABS(YDD)
      IF (YDA.LE.ERR) GO TO 101
      IF (N.GE.10) GO TO 101
      YE=1.-YDA**0.25
      YDC=YDA**YE
      PHI(2)=PHI(2)*(1.+SIGN(YDC,YDD))
      GO TO 100
101 IF (KD.EQ.0) ISTOP=M2
      PRINT 20, N,YD,SCOPE,DEPTH
      20 FORMAT (1H1,*THIS IS THE RESULTS AT ITERATION NUMBER=*,I4,*)

```

```

WATER DEPTH=*,F8.2////
19X,*X*,14X,*Y*,9X,*ELONG. LENGTH*,6X,*FORCE*,8X,*FORCE/U.F.*,5X,*LL
LONGATION*,5X,*ANGLE TO Y*,9X,*I*)
PRINT 30, (X(I),Y(I),Z(I),F(I),K(I),Z(I),PHI(I),I, I=2,1STOP,NN)
PRINT 30, X(M2),Y(M2),Z(M2),F(M2),K(M2),Z(M2),PHI(M2),M2
30 FORMAT(7E15.4,I10)
2000 CONTINUE
STOP
END

```

# EXAMPLE OF DATA INPUT

```

1 3
44. 0.16 0.008 1.5 0.5
4.5 30. 2.1 .264
4.5 30. 2.1 .264
0. 0. 0. 0.
30. 10000. .002
0. 53000.
30. 1.5 53000. 0.063 0. 0
8850. 1.5 53000. 0.063 0. 0
210. 1.5 53000. 0.063 0. 0
10

```

## APPENDIX D. Program DYN SIN

### D.1 Purpose

To obtain dynamic mooring line tension under sine wave.

### D.2 Program Logic

The program starts with a set of assumed equivalent linear damping coefficients to solve (19) and obtain the response quantities. The corrected damping coefficients are calculated from (B.25) and (B.27) and then compared with the assumed values. If the differences are not within the allowable limit, the new damping coefficients are introduced and the program repeated. The convergence is ensured because a higher damping will result in a lower velocity response; and a lower damping, a higher velocity response. The coefficients converge rapidly.

### D.3 Notations

#### (A) Input

NLK	Number of cases
K	Number of line sections
E	Material elastic constant (see Table 1.) in psf.
EO	Material elastic constant (see Table 1.) in psf.
Q	Material visco-elastic constant (see Table 1.) in foot-pound-second system
L	Length of the line section in feet.
DI	Diameter of the rope in inches
Z	Mooring line strain under steady state tension.
RO	Mass of the rope (including the entrained water) per unit length in slug/ft.
FM	Mass of the package (including the virtual mass) in slug

LP Length of the package in feet  
 CD Hydrodynamic drag of the package acting in the axial direction  
 MC Material code: MC = 0 for fiber rope; MC = 1 for wire rope  
 MM Material model code: MM = 1, 2, 3, 4 (see Table 1.)  
 HS Significant wave height in feet  
 XINCW The length of the nylon line in which the variation of the velocity amplitude can be approximated by linear rule.  
 XINCS Same as above for wire rope  
 CDT Tangential hydrodynamic drag coefficient on the rope surface  
 UAP Assumed linearization factor of the water drag on the package  
 DCR Assumed linerization factor of the water drag on the rope surface

(B) Output

UA Displacement amplitude in feet  
 SIGMA Mooring line force amplitude in pounds  
 LT Total length of the mooring line from the buoy in feet  
 I Index

D.4 Remarks

(1) The number of line sections is limited to 10. It can be enlarged by changing the program dimensions. The program requires a core capacity of 60 K.

(2) The program handles four types of material models as listed in Table 1.

- (3) Virtual packages may be inserted in the mooring line.
- (4) It takes a few seconds to obtain the results of a 3-section mooring line with a water depth of 10,000 feet (compilation time excluded).

#### D.5 Program Listing

```

PROGRAM DYNIN(INPUT,OUTPUT,TAPE5=INPUT,TAPE6=OUTPUT)
  DIMENSION A(38,38),L(10),DI(10),RO(10),L(10),PM(10),      SP(10),
  IAE(10),SS(10),SC(10),CS(10),CC(10),WK(10),WSP(10),Z(10),      LT(6
  10),UA(60),MC(10),B(40),SIGMA(60),LS(10),LP(10),W(10),CD(10),ALP(10
  1),BEI(10),WW(10),WE(10),AEA(10),AEB(10),AWA(10),AWB(10),UAP(10),
  IAW(10),CDI(10),CDK(10),UAPC(10),UAPS(10),DCR(10),DCKC(10),DCNS(10)
  1,MM(10),EO(10),MC(10)
  REAL L,LI,LD,LINCK,LP,LS
  READ 10, NLK
10  FORMAT (I4)
  DO 6000 NL=1,NLK
    READ 10, K
    KD=K-1      KDD=K-2
    NRB=4*K-2
    NCB=NRB
    READ 12,(E(I),EO(I),W(I),L(I),DI(I),Z(I),RO(I),PM(I),LP(I),CD(I),
    1C(I),MM(I), I=1,K)
12  FORMAT (3F10.0,7F6.0,2I4)
    PRINT 32
32  FORMAT (1H1,3X,*E(I)*,7X,*EO(I)*,6X,*W(I)*,7X,*DI(I)*,6X,*Z(I)*,7X,
  1*RO(I)*,6X,*L(I)*,7X,*PM(I)*,6X,*LP(I)*,6X,*CD(I)*,3X,*MC(I)*,*
  1(I)*,*      1*)
    PRINT 22,(E(I),EO(I),W(I),DI(I),Z(I),RO(I),L(I),PM(I),LP(I),CD(I),
    1MC(I),MM(I),I,I=1,K)
22  FORMAT (1H ,10E11.4,3I5)
    DO 180 J=1,K
      DI(J)=DI(J)/SQRT(1.+Z(J))/12.
180  CONTINUE
    READ 16, HS,T,XINCN,XINCS,CDT
16  FORMAT (5F6.0)
    PRINT 29, HS,T,XINCN,XINCS,CDT
29  FORMAT (*      HS=*,F4.1,*      T=*,F4.1,*      XINCN=*,F5.0,*      XI
  1NCS=*,F5.0,*      CDT=*,F5.3)
    W=6.2832/T
    WS=W*W
    READ 18,(UAP(I),I=1,KD)
18  FORMAT (10F8.0)
    READ 17,(DCR(I), I=1,K)
17  FORMAT (10F6.0)
    READ 10, NN
    NIT=0
4000 IF (NIT.GE.6) GO TO 4010
    NIT=NIT+1
    DO 100 I=1,NRB
    DO 150 J=1,NCB
150  A(I,J)=0.
100  CONTINUE
    DO 200 J=1,K
      IF (MM(J).EQ.1) GO TO 111
      IF (MM(J).EQ.3) GO TO 113
      IF (MM(J).EQ.4) GO TO 114
      GO TO 115
111  Q(J)=Q(J)*W
      GO TO 115
113  QEO=Q(J)/EO(J)
      QWS=1.+WS*QEO**2

```

```

E(J)=E(J)+EU(J)*WS*WEU**2/WS
Q(J)=Q(J)*W/WS
GO TO 115
114 EQS=EU(J)**2+Q(J)**2
E(J)=E(J)+EU(J)/EQS
Q(J)=EU(J)**2*Q(J)/EQS
115 AR=.7854*DI(J)*DI(J)
AR=.7854*DI(J)*DI(J)
AE(J)=AR *E(J)
AQ(J)=AR*Q(J)
SP(J)=SQRT(E(J)/RQ(J))
WSP(J)=W/SP(J)
WSPS=WSP(J)**2
LS(J)=L(J)*(1.+Z(J))
QE(J)=G(J)/E(J)
QES=QE(J)**2
CDP(J)=.848*CD(J)*UAP(J)*W
CDR(J)=2.6667*DI(J)*W*DCR(J)*CDT/AE(J)
QEW=QE(J)*CDR(J)*W
GA=WSPS-QEW
GAS=GA*GA
GB=CDR(J)*W+QE(J)*WSPS
GBS=GB*GB
GC=SQRT(GAS+GBS)
GD=2.*(1.+QES)
ALP(J)=SQRT((GA+GC)/GD)
BET(J)=-SQRT((-GA+GC)/GD)
ALPL=ALP(J)*LS(J)
BETL=BET(J)*LS(J)
SINH=(EXP(BETL)-EXP(-BETL))/2.
COSH=(EXP(BETL)+EXP(-BETL))/2.
SS(J)=SIN(ALPL)*SINH
SC(J)=SIN(ALPL)*COSH
CS(J)=COS(ALPL)*SINH
CC(J)=COS(ALPL)*COSH
AEA(J)=AE(J)*ALP(J)
AEB(J)=AE(J)*BET(J)
AQA(J)=AQ(J)*ALP(J)
AQB(J)=AQ(J)*BET(J)
200 CONTINUE
DO 300 I=1,K
J=4*I-3      $      JJ=J+1
A(J,J)=SC(I)      $      A(JJ,JJ)=SC(I)
300 CONTINUE
DO 400 I=1,K
J=4*I-2      $      JJ=J-1
A(J,JJ)=CS(I)      $      A(JJ,J)=-CS(I)
400 CONTINUE
IF (KD.LE.0) GO TO 1030
DO 500 I=1,KD
J=4*I-3      $      JJ=J+2
A(J,JJ)=CC(I)      $      A(J+1,JJ+1)=CC(I)
500 CONTINUE
DO 600 I=1,KD
JJ=4*I      $      J=JJ-3
A(J,JJ)=SS(I)      $      A(J+1,JJ-1)=-SS(I)

```



```

600 CONTINUE
DO 700 I=1,KD
  J=4*I+1      JJ=J-2
  A(J,JJ)=-1.   A(J+1,JJ+1)=-1.
700 CONTINUE
DO 800 I=1,KD
  J=4*I-1      JK=J+1
  IO=I+1
  A(J,J-2)=AQB(I)-AEA(I)
  A(J,J-1)= AEB(I)+AWA(I)
  A(J,J )=-FPA(I)*WS
  A(J,J+1)=-CDP(I)*W
  A(J,J+2)=(AEA(I+1)-AQB(I+1))*CC(I+1)+(AEB(I+1)+AWA(I+1))*SS(I+1)
  A(J,J+3)=(AEA(I+1)-AQB(I+1))*CS(I+1)-(AEB(I+1)+AWA(I+1))*CC(I+1)
  A(J+1,J-2)=-A(J,J-1)
  A(J+1,J-1)=A(J,J-2)
  A(J+1,J )=-A(J,J+1)
  A(J+1,J+1)=A(J,J)
  A(J+1,J+2)=(AEB(IO)+AWA(IO))*CC(IO)+(AQB(IO)-AEA(IO))*SS(IO)
  A(J+1,J+3)=(AEB(IO)+AWA(IO))*CS(IO)-(AQB(IO)-AEA(IO))*CC(IO)
800 CONTINUE
IF (KDD.LE.0) GO TO 1030
DO 900 I=1,KDD
  J=4*I      IO=I+1
  JK=J-1
  A(JK,J+3)=(AEB(IO)+AWA(IO))*CS(IO)+(AQB(IO)-AEA(IO))*SC(IO)
  A(JK,J+4)=(AEB(IO)+AWA(IO))*SC(IO)-(AQB(IO)-AEA(IO))*CS(IO)
  A(J,J+3)=(-AEA(IO)+AQB(IO))*CS(IO)-(AEB(IO)+AWA(IO))*SC(IO)
  A(J,J+4)=(-AEA(IO)+AQB(IO))*SC(IO)+(AEB(IO)+AWA(IO))*CS(IO)
900 CONTINUE
1030 DO 1050 I=1,NRB
  B(I)=0.
1050 CONTINUE
  B(1)=HS/2.
  N=NRB
  M=1
  ISIZE=38
  JSIZE=NCB
  CALL INVK(A, N,B, M,DEFLEN,ISIZE,JSIZE)
  K4=4*K      K3=K4-1
  B(K4)=0.     B(K3)=0.
C PRINT 50, (B(I),I=1,K4)
5. FORMAT (12E10.2)
N=1
LT(1)=0.
DO 1100 I=1,K
  U2X=0.
  U3X=0.
  JL=0
  JK=4*I      JJ=JK-1
  JI=JK-2     JH=JK-3
  C1=B(JI)*SC(I)+B(JK)*CC(I)+B(JH)*CS(I)-B(JJ)*SS(I)
  C2=B(JJ)*CC(I)+B(JK)*SS(I)+B(JH)*SC(I)-B(JI)*CS(I)
  JA(N)=SGRI(C1+C2*C2)
  AJS=7*EA(I)*CS(I)
  ACC=A(A(I))*CC(I)

```

```

ASC=AEA(I)*SC(I)
ACS=AEA(I)*CS(I)
BSS=AEB(I)*SS(I)
BSC=AEB(I)*SC(I)
BCC=AEB(I)*CC(I)
BCS=ALB(I)*CS(I)
C4=B(JI)*(ASS-BCC)+B(JK)*(BSC+ACS)+B(JH)*(BSS+ACC)+B(JJ)*(BCS-ASC)
C3=B(JI)*(ACC+BSS)+B(JK)*(BCS-ASC)+B(JH)*(BCC-ASS)-B(JJ)*(BSC+ACS)
C5=C4-QE(I)*C3
C6=C3+QE(I)*C4
SIGMA(N)=SQRT(C5*C5+C6*C6)
IF (MC(I).EQ.1) GO TO 1210
XINC=XINCN
GO TO 1220
1210 XINC=XINCS
1220 XINCS=XINC*(1.+Z(I))
IF (L(I).LE.XINC) GO TO 1200
JD=IFIX(L(I)/XINC)
DO 1150 J=1,JD
N=N+1
LT(N)=LT(N-1)+XINCS
X=LS(I)-XINCS*FLOAT(J)
ALPX=ALP(I)*X
BETX=BET(I)*X
EXB=EXP(BETX)      EXBN=EXP(-BETX)
SINHx=(EXB-EXBN)/2.
COSHx=(EXB+EXBN)/2.
SSX=SIN(ALPX)*SINHx
SCX=SIN(ALPX)*COSHx
CSX=COS(ALPX)*SINHx
CCX=COS(ALPX)*COSHx
C1=B(JI)*SCX +B(JK)*CCX +B(JH)*CSX -B(JJ)*SSX
C2=B(JJ)*CCX +B(JK)*SSX +B(JH)*SCX -B(JI)*CSX
UA(N)=SQRT(C1*C1+C2*C2)
ASS=ALP(I)*SSX
ACC=ALP(I)*CCX
ASC=ALP(I)*SCX
ACS=ALP(I)*CSX
BSS=BET(I)*SSX
BSC=BET(I)*SCX
BCC=BET(I)*CCX
BCS=BET(I)*CSX
C3=B(JI)*(ACC+BSS)+B(JK)*(BCS-ASC)+B(JH)*(BCC-ASS)-B(JJ)*(BSC+ACS)
C4=B(JI)*(ASS-BCC)+B(JK)*(BSC+ACS)+B(JH)*(BSS+ACC)+B(JJ)*(BCS-ASC)
C5=C4-QE(I)*C3
C6=C3+QE(I)*C4
SIGMA(N)=SQRT(C5*C5+C6*C6)*AE(I)
UD=(UA(N)-UA(N-1))/JA(N-1)
JDS=UD*UD
JAS=UA(N-1)*JA(N-1)
U2X=U2X+JAS*XINCS*(1.+UD+UD*UD/3.)
U3X=U3X+UAS*UA(N-1)*XINCS*(1.+1.5*UD+UD*UD+UD*UD*UD/4.)
1150 CONTINUE
1200 N=N+1
NJD=N-JD-1
LT(N)=LS(I)+LT(NJD)

```

```

      UA(N)=SQRT(B(JK)*B(JK)+B(JJ)*B(JJ))
      UAPC(I)=UA(N)
      UAPS(I)=(UAP(I)-UAPC(I))/UAP(I)
      C3=B(JI)*ALP(I)+B(JH)*BET(I)
      C4=-B(JI)*BET(I)+B(JH)*ALP(I)
      C5=C4-QE(I)*C3
      C6=C3+QE(I)*C4
      SIGMA(N)=SQRT(C5*C5+C6*C6)*AL(I)
      LINCR=LT(N)-LI(N-1)
      UD=(UA(N)-UA(N-1))/UA(N-1)
      UDS=UD*UD
      UAS=UA(N-1)*UA(N-1)
      U2X=U2X+UAS*LINCR*(1.+UD+UDS/3.)
      U3X=U3X+UAS*UA(N-1)*LINCR*(1.+1.5*UD+UDS+UDS*UD/4.)
      N=N+1
      LT(N)=LT(N-1)+LP(I)
      DCKC(I)=U3X/U2X
      DCKS(I)=(DCKC(I)-DCK(I))/DCK(I)
1100 CONTINUE
C      PRINT 26, (DCK(I),DCKC(I),DCKS(I), I=1,K)
      26 FORMAT (9E13.5)
      DO 3050 I=1,K
      DCR(I)=DCKC(I)
3050 CONTINUE
      DO 3030 I=1,KD
      UAP(I)=(UAP(I)+UAPC(I))/2.
      UAPS(I)=UAP(I)/UAPC(I)-1.
3030 CONTINUE
C
C      ALLOWABLE ERROR FOR DCR IS 10 PERCENT
C
      DO 3080 I=1,K
      IF (ABS(DCKS(I)).GT.0.1) GO TO 4000
3080 CONTINUE
C
C      ALLOWABLE ERROR FOR UAP IS 20 PERCENT
C
      DO 3090 I=1,KD
      IF (ABS(UAPS(I)).GE.0.2) GO TO 4000
3090 CONTINUE
4010 NH=N-1
      PRINT 80, (DCR(I), I=1,K)
      80 FORMAT (1H,////5X,*DCR(1)*,4X,*DCR(2)*,4X,*DCR(3)*,4X,*DCR(4)*,4X
1,*DCR(5)*,4X,*DCR(6)*,4X,*DCR(7)*,4X,*DCR(8)*,4X,*DCR(9)*,4X,*DCR(
11)**//((F10.2))
      PRINT 84, (UAP(I), I=1,KD)
      84 FORMAT (1H,////5X,*UAP(1)*,4X,*UAP(2)*,4X,*UAP(3)*,4X,*UAP(4)*,4X
1,*UAP(5)*,4X,*UAP(6)*,4X,*UAP(7)*,4X,*UAP(8)*,4X,*UAP(9)*,4X,*UAP(
11)**//((F10.2))
      PRINT 60,N,NIT
      60 FORMAT (1H,/////////* THIS IS THE RESULTS WITH DAMPING AT FREQ
1UENCY=*,F6.6,* NUMBER OF ITERATION=*,I2////////9X,*CA*,12X,*SIGM
1A*,14X,*LI*,1X,*I*)
      PRINT 70, (UA(I),SIGMA(I),LT(I),I, I=1,NH,NH)
      70 FORMAT(3E15.4,I10)
6000 CONTINUE

```

```

      STOP
      END
      SUBROUTINE INVR(A,N,D,M,DETERM,ISIZE,JSIZE)
      DIMENSION IPIVOT(100),A(ISIZE,JSIZE),B(ISIZE,M),INDEX(100,2),
      IPIVOT(100)
      EQUIVALENCE (IROW,JROW),(ICOL,JCOL),(AMAX,I,SWAP)
C
      10 DETERM=1.0
      15 DO 20 J=1,N
      20 IPIVOT(J)=0
      30 DO 550 I=1,N
C
C      SEARCH FOR PIVOT ELEMENT
C
      40 AMAX=0.0
      45 DO 105 J=1,N
      50 IF (IPIVOT(J)-1) 60,105.00
      60 DO 100 K=1,N
      70 IF (IPIVOT(K)-1) 80,100.740
      80 IF (ABS(AMAX)-ABS(A(J,K))) 85,100,100
      85 IROW=J
      90 ICOL=K
      95 AMAX=A(J,K)
      100 CONTINUE
      105 CONTINUE
      110 IPIVOT(ICOL)=IPIVOT(ICOL)+1
C
C      INTERCHANGE ROWS TO PUT PIVOT ELEMENT ON DIAGONAL
C
      130 IF (IROW-ICOL) 140, 260, 140
      140 DETERM=-DETERM
      150 DO 200 L=1,N
      160 SWAP=A(IROW,L)
      170 A(IROW,L)=A(ICOL,L)
      200 A(ICOL,L)=SWAP
      205 IF(M) 260, 260, 210
      210 DO 250 L=1,M
      220 SWAP=B(IROW,L)
      230 B(IROW,L)=B(ICOL,L)
      250 B(ICOL,L)=SWAP
      260 INDEX(1,1)=IROW
      270 INDEX(1,2)=ICOL
      310 PIVOT(1)=A(ICOL,ICOL)
      320 DETERM=DETERM*PIVOT(1)
C
C      DIVIDE PIVOT ROW BY PIVOT ELEMENT
C
      330 A(ICOL,ICOL)=1.0
      340 DO 350 L=1,N
      350 A(ICOL,L)=A(ICOL,L)/PIVOT(1)
      355 IF(M) 380, 380, 360
      360 DO 370 L=1,M
      370 B(ICOL,L)=B(ICOL,L)/PIVOT(1)
C
C      REDUCE NON-PIVOT ROWS
C

```

```

380 DO 550 L=1,N
390 IF (LJ-ICOLU) 400,550,450
400 I=A(L1,ICOLU)
420 A(L1,ICOLU)=0.0
430 DO 450 L=1,N
450 A(L1,L)=A(L1,L)-A(1(1COLU),L)*I
455 IF (M) 550,550,460
460 DO 500 L=1,M
500 B(L1,L)=B(L1,L)-B(1COLU,L)*I
550 CONTINUE
C
C   INTERCHANG COLUMNS
C
600 DO 710 I=1,N
610 L=N+1-I
620 IF (INDEX(L,1)-INDEX(L,2)) 630,710,650
630 JROW=INDEX(L,1)
640 JCOLUM=INDEX(L,2)
650 DO 705 K=1,N
660 S=AP=A(K,JROW)
670 A(K,JROW)=A(K,JCOLUM)
700 A(K,JCOLUM)=S=AP
705 CONTINUE
710 CONTINUE
740 RETURN
END

```

# EXAMPLE OF DATA INPUT

```

1
3
50240000.    0.    4000000.    30.    1.0    .1019    2.    4.    4.0    .27    0
50240000.    0.    4000000.    3000.    1.0    .0999    2.    4.    4.0    .27    0
50240000.    0.    4000000.    210.    1.0    .0999    2.
10.    5.2 1.0.    1000. 0.013
4.98    .33
4.90    4.61    .25
1

```

## APPENDIX E. Program DYNRAN

### E.1 Purpose

To obtain the dynamic mooring mooring line tension under random waves.

### E.2 Program Logic

Same as DYN SIN except the corrected damping coefficients are calculated from (24) and (25).

### E.3 Notations

#### (A) Input

Same as in Appendix D, plus

F Frequency, in cycles/sec.

KW Number of frequencies considered

NSPEC Wave spectrum code:

NSPEC = 1 for Pierson and Moskowitz's spectrum

NSPEC = 2 for Scott's spectrum

#### (B) Output

UA Displacement amplitude under unit Sine wave excitation

USPEC  $(UA)^2 \cdot S_{hh}(f) \cdot \Delta f$ ;  $S_{hh}(f)$  is the buoy motion spectrum

EBSILO Strain amplitude under unit Sine wave excitation

ESPEC  $(EBSILO)^2 S_{hh}(f) \Delta f$

SIGMA Force amplitude under unit Sine wave excitation

TSPEC  $(SIGMA)^2 S_{hh}(f) \Delta f$

LT Mooring line position from the buoy

UVAR Variance of the displacement  $\sigma_u^2$ ; in (lbs.)<sup>2</sup>

EVAR Variance of the strain  $\sigma_\epsilon^2$

TVAR Variance of the dynamic force  $\sigma_t^2$ ; in (lbs.)<sup>2</sup>

TM2  $\int_0^\infty \omega^2 S_{tt}(\omega) d\omega$ ;  $S_{tt}(\omega)$  is the force spectrum

$$TM4 \quad \int_0^{\infty} \omega^4 S_{tt}(\omega) d\omega$$

TEB The band width indicator

I Position index

$$VSAR \quad \int_0^L \sigma_V^2 dX; \quad V \text{ is the velocity}$$

$$VTAR \quad \int_0^L \sigma_V^3 dX.$$

DCRC Corrected linearization factor of the mooring rope

UAPC Corrected linearization factor of the package.

$$DCRD \quad DCRD = DCRC/DCR - 1$$

$$UAPD \quad UAPD = UAPC/UAP - 1$$

$$DCRS \quad DCRS = \sum_{1}^K (DCRD)^2$$

$$UAPS \quad UAPS = \sum_{1}^K (UAPD)^2$$

#### E.4 Remarks

(1), (2), (3), and (4) same as in Appendix D.

(5) If the linearization factors do not converge to the acceptable values in six iterations, the operation passes to another case.

(6) The frequency may be arbitrarily spaced.

#### E.5 Program Listing

```

PROGRAM DYKRAH(INPUT,OUTPUT,TAPL5=INPUT,TAPL6=OUTPUT)
DIMENSION A(38,38),E(10),DI(10),RO(10),L(10),PM(10), SP(10),
IAF(10),CS(10),SC(10),CB(10),CC(10),WK(10),WSP(10),Z(10),F(20),LI(6
10),UA(60),MC(10),BI(40),SIGMA(60),LS(10),LP(10),W(10),CD(10),ALP(10
10),BFT(10),WW(10),WF(10),AFA(10),AEB(10),AWA(10),AWB(10),CAP(10),
IAZ(10),CDP(10),CDK(10),UAPC(10), DCR(10),EU(10),MM(10),VOP
1EC(60),VVAR(60),VAS(20),UAPD(10),DCNC(10),DCND(10),VSAK(10),VIAK(1
10),KE(10),KI(10),ISP(C(60),OSPEC(60),EBSILO(60),ESPEC(60),UVAR(60)
1,EVAR(60),IVAR(60),IM2(60),IM4(60),TEB(60)
REAL L,LI,LD,LINCK,LP,LS
131 FORMAT (14E12.4,I10)
READ 10,NLK,K
14 FORMAT (2I4)
DO 60 J=1,NLK
READ 12,(F(1),F0(1),W(1),L(1),DI(1),Z(1),RO(1),PM(1),LP(1),CD(1),M
1C(1),MM(1), I=1,K)
12 FORMAT (3F10.0,7F6.0,2I4)
PRINT 32
32 FORMAT (1H1,3X,*E(1)^,7X,*EO(1)^,6X,*W(1)^,7X,*DI(1)^,6X,*Z(1)^,7X,
1*RO(1)^,6X,*L(1)^,7X,*PM(1)^,6X,*LP(1)^,6X,*CD(1)^,3X,*MC(1)^,*
1(1)^,* I*)
PRINT 22,(F(1),EO(1),W(1),DI(1),Z(1),RO(1),L(1),PM(1),LP(1),CD(1),
1MC(1),MM(1), I=1,K)
22 FORMAT (1H ,14E11.4,3I5)
DO 180 J=1,K
DI(J)=DI(0)/COSK(1.+Z(J))/12.
180 CONTINUE
K0=K-1 1 KDD=K-2
NRB=4*K-2
NCB=NPB
READ 5, K4
5 FORMAT (I4)
READ 14, (F(I), I=1,K4)
14 FORMAT (20F4.0)
READ 16, H0,XINC0,XINC3,CDI,NSPEC
16 FORMAT (4F6.0,I4)
PRINT 26, H0,XINC0,XINC3,CDI,NSPEC
26 FORMAT (1H ,H0=*,F6.2,* XINC0=*,F6.1,* XINC3=*,F6.1,*
1 CDI=*,F6.3,* NSPEC=*,I2)
READ 18, (UAP(I), I=1,K0)
18 FORMAT (10F8.0)
READ 17, (DCR(I), I=1,K)
17 FORMAT (10F6.0)
PRINT 27,K
27 FORMAT (* DCR(I) FROM 1 TO K 14)
PRINT 37, (DCR(I), I=1,K)
PRINT 28,K0
28 FORMAT (* UAP(I) FROM 1 TO K, 14)
PRINT 37, (UAP(I), I=1,K0)
37 FORMAT (10E12.3)
DO 103 I=1,60
UVAR(I)=0.
FVAR(I)=0.
IVAR(I)=0.
IM2(I)=0.
IM4(I)=0.

```



```

193 CONTINUE
  IF (NSPEC.EQ.2) GO TO 94
  IF (HS.GE.24.) HS=J*.27*(HS+5.8)**2
94 DFC=0.
  KNN=Kw-1
  DO 128 IK=1,Kw
    DFA=F(IK)+F(IK+1)
    DF=DFA/2.-DFC
    DFC=DFC+DF
    W=F(IK)*6.2832
    WS=W*W
    DW=DF*6.2832
    IF (NSPEC.EQ.2) GO TO 126
    UAT=(.0053885/F(IK)**5)*EXP(-.02132/HS**2/F(IK)**4)
    UAS(IK)=UAT*DF
    GO TO 128
126 W=1./(0.03*HS+1.35)
    WW=W-W(0.26)
    IF (WW.LE.0.) GO TO 127
    WE=SQR((WW-0.26)**2/(.065/WW))
    UAT=.0214*HS*HS*EXP(-WE)
    UAS(IK)=UAT*DW
    GO TO 128
127 UAS(IK)=0.
128 CONTINUE
C   PRINT 134,(F(J),UAS(J),J=1,KNN)
134 FORMAT (2F14.4)
  NIT=0
  NKK=0
2001 DO 93 I=1,60
  VVAR(I)=0.
  93 CONTINUE
  DO 200 IK=1,KNN
    W=F(IK)*6.2832
    WS=W*W
    DO 100 I=1,NRR
    DO 150 J=1,NCR
150 A(I,J)=0.
100 CONTINUE
  DO 200 J=1,K
    IF (MM(J).EQ.1) GO TO 111
    IF (MM(J).EQ.3) GO TO 113
    IF (MM(J).EQ.4) GO TO 114
    GO TO 115
111 Q(J)=Q(J)*W
    GO TO 115
113 QEO=Q(J)/EO(J)
    QAS=1.+WS*QEO**2
    L(J)=E(J)+EO(J)*WS*QEO**2/WS
    J(J)=Q(J)*W/WS
    GO TO 115
114 EQS=E(J)**2+Q(J)**2
    F(J)=E(J)+EQ(J)/EQS
    Q(J)=F(J)**2*Q(J)/EQS
115 AR=.7854*DI(J)*DI(J)
    AE(J)=AR *E(J)

```

```

AQ(J)=AR*Q(J)
SP(J)=SQRT(E(J)/RO(J))
WSP(J)=R/SP(J)
WSP5=WSP(J)**2
LS(J)=L(J)*(1.+Z(J))
QE(J)=Q(J)/F(J)
QE5=QE(J)**2
CDP(J)=J.9*CD(J)*CAP(J)
CDR(J)=2.8284*D1(J)*DCK(J)*CD1/AE(J)
QEW=QE(J)*CDR(J)*W
GA=WSP5-QEW
GAS=GA*GA
GB=CDR(J)*W+QE(J)*WSP5
GB5=GB*GB
GC=SQRT(GAS+GB5)
GD=2.*(1.+QE5)
ALP(J)=SQRT((GA+GC)/GD)
BET(J)=-SQRT(ABS(-GA+GC)/GD)
ALPL=ALP(J)*LS(J)
BETL=BET(J)*LS(J)
SINH=(EXP(BETL)-EXP(-BETL))/2.
COSH=(EXP(BETL)+EXP(-BETL))/2.
JS(J)=SIN(ALPL)*SINH
JL(J)=SIN(ALPL)*COSH
CS(J)=COS(ALPL)*SINH
CC(J)=COS(ALPL)*COSH
AFA(J)=AF(J)*ALP(J)
AEP(J)=AE(J)*BET(J)
AQA(J)=AQ(J)*ALP(J)
AQB(J)=AQ(J)*BET(J)
200 CONTINUE
DO 300 I=1,K
J=4*I-3 JJ=J+1
A(J,J)=SC(I) A(JJ,JJ)=SC(I)
300 CONTINUE
DO 400 I=1,K
J=4*I-2 JJ=J-1
A(J,JJ)=CC(I) A(JJ,J)=-C(J)
400 CONTINUE
IF (ND.LF.0) GO TO 1030
DO 500 I=1,KD
J=4*I-3 JJ=J+2
A(J,JJ)=CC(I) A(J+1,JJ+1)=CC(I)
500 CONTINUE
DO 600 I=1,KD
JJ=4*I JJ=JJ-3
A(J,JJ)=JS(I) A(J+1,JJ-1)=-JS(I)
600 CONTINUE
DO 700 I=1,KD
J=4*I+1 JJ=J-2
A(J,JJ)=-1. A(J+1,JJ+1)=-1.
700 CONTINUE
DO 800 I=1,KD
J=4*I-1 JK=J+1
IO=I+1
A(J,J-2)=AQB(I)-AFA(I)

```

```

A(J,J-1)=AEB(I)+AWA(I)
A(J,J)=-PM(I)*WS
A(J,J+1)=-CDP(I)*W
A(J,J+2)=(AFA(I+1)-AWB(I+1))*CC(I+1)+(AEB(I+1)+AWA(I+1))*SS(I+1)
A(J,J+3)=(AFA(I+1)-AWB(I+1))*SS(I+1)-(AEB(I+1)+AWA(I+1))*CC(I+1)
A(J+1,J-2)=-A(J,J-1)
A(J+1,J-1)=A(J,J-2)
A(J+1,J)=-A(J,J+1)
A(J+1,J+1)=A(J,J)
A(J+1,J+2)=(AEB(I0)+AWA(I0))*CC(I0)+(AWB(I0)-AEA(I0))*SS(I0)
A(J+1,J+3)=(AEB(I0)+AWA(I0))*SS(I0)-(AWB(I0)-AEA(I0))*CC(I0)
800 CONTINUE
IF (KDD.LE.0) GO TO 1030
DO 900 I=1,KDD
J=4*I  B I0=I+1
JK=J-1
A(JK,J+3)=(AEB(I0)+AWA(I0))*CS(I0)+(AWB(I0)-AEA(I0))*SC(I0)
A(JK,J+4)=(AEB(I0)+AWA(I0))*SC(I0)-(AWB(I0)-AEA(I0))*CS(I0)
A(J,J+3)=(-AEA(I0)+AWB(I0))*CS(I0)-(AEB(I0)+AWA(I0))*SC(I0)
A(J,J+4)=(-AEA(I0)+AWB(I0))*SC(I0)+(AEB(I0)+AWA(I0))*CS(I0)
900 CONTINUE
1030 CONTINUE
DO 1050 I=1,NRB
B(I)=0.
1050 CONTINUE
B(1)=1.
N=NRB
M=1
ISIZE=38
JSIZE=NCB
CALL INVR(A, N,B, M,DETERM,ISIZE,JSIZE)
K4=4*K  B K3=K4-1
B(K4)=0.  B B(K3)=0.
C PRINT 5, (B(I),I=1,K4)
5. FORMAT (12E10.2)
N=1
LI(1)=0.
DO 1100 I=1,K
KI(I)=N
JD=-
JK=4*I  B JJ=JK-1
JI=JK-2  B JH=JK-3
C1=B(JI)*SC(I)+B(JK)*CC(I)+B(JH)*CS(I)-B(JJ)*SS(I)
C2=B(JJ)*CC(I)+B(JK)*SS(I)+B(JH)*SC(I)-B(JI)*CS(I)
JA(N)=SQRT(C1**2+C2**2)
VSPEC(N)=WS*UA(N)**2*UAS(IK)
VVAR(N)=VVAR(N)+VSPEC(N)
IF (NKK.EQ.0) GO TO 1800
USPEC(N)=UA(N)**2*UAS(IK)
UVAR(N)=UVAR(N)+USPEC(N)
ASS=AFA(I)*CS(I)
ACC=AEA(I)*CC(I)
ASC=AEA(I)*SC(I)
ACS=AEA(I)*CS(I)
BSS=AEB(I)*SS(I)
BSC=AEB(I)*SC(I)

```

```

BCC=AEH(I)*(C(I)
BCS=AEH(I)*C5(I)
C4=B(JI)*(ASS-BCC)+B(JK)*(BSC+ACS)+B(JH)*(BSS+ACC)+B(JJ)*(BCS-ASC)
C3=B(JI)*(ACC+BSS)+B(JK)*(BCS-ASC)+B(JH)*(BCC-ASS)-B(JJ)*(BSC+ACS)
C5=C4-QE(I)*C3
C6=C3+QE(I)*C4
EB3ILO(N)=SQRT(C3*C3+C4*C4)/AE(I)
ESPEC(N)=EB3ILO(N)**2*UAS(IK)
EVAR(N)=EVAR(N)+ESPEC(N)
SIGMA(N)=SQRT(C5*C5+C6*C6)
TSPEC(N)=SIGMA(N)**2*UAS(IK)
TVAR(N)=TVAR(N)+TSPEC(N)
TM2(N)=TM2(N)+TSPEC(N)*WS
TM4(N)=TM4(N)+TSPEC(N)*WS*WS
C PRINT 131,ALP(I),BET(I),X,C3,C4,C5,C6,AE(I),QE(I),SIGMA(N),N
1800 IF (MC(I).EQ.1) GO TO 1210
XINC=XINC+
GO TO 1220
1210 XINC=XINC+
1220 XINCS=XINC*(1.+Z(I))
IF (L(I).LE.XINC) GO TO 1200
JD=FIX(L(I)/XINC)
DO 1150 J=1,JD
N=N+1
LT(N)=LT(N-1)+XINCS
X=LS(I)-XINCS*FLUAT(J)
ALPX=ALP(I)*X
BETX=BET(I)*X
EXB=EXP(BLTX) * EXBN=EXP(-BETX)
SINHx=(EXB-EXBN)/2.
COSHx=(EXB+EXBN)/2.
SSX=SIN(ALPX)*SINHx
SCX=SIN(ALPX)*COSHx
CSX=COS(ALPX)*SINHx
CCX=COS(ALPX)*COSHx
C1=B(JI)*SCX +B(JK)*CCX +B(JH)*CSX -B(JJ)*SSX
C2=B(JJ)*CCX +B(JK)*SSX +B(JH)*SCX -B(JI)*CSX
UA(N)=SQRT(C1*C1+C2*C2)
VSPEC(N)=WS*UA(N)**2*UAS(IK)
VVAR(N)=VVAR(N)+VSPEC(N)
IF (NKK.EQ.0) GO TO 1150
USPEC(N)=UA(N)**2*UAS(IK)
UVAR(N)=UVAR(N)+USPEC(N)
ASS=ALP(I)*SSX
ACC=ALP(I)*CCX
ASC=ALP(I)*SCX
ACS=ALP(I)*CSX
BSS=BET(I)*SSX
BSC=BET(I)*SCX
BCC=BET(I)*CCX
BCS=BET(I)*CSX
C3=B(JI)*(ACC+BSS)+B(JK)*(BCS-ASC)+B(JH)*(BCC-ASS)-B(JJ)*(BSC+ACS)
C4=B(JI)*(ASS-BCC)+B(JK)*(BSC+ACS)+B(JH)*(BSS+ACC)+B(JJ)*(BCS-ASC)
C5=C4-QE(I)*C3
C6=C3+QE(I)*C4
EB3ILO(N)=SQRT(C3*C3+C4*C4)

```

```

    TSPEC(N)=LDSILO(N)**2*UAS(IK)
    EVAR(N)=EVAR(N)+ESPEC(N)
    SIGMA(N)=SQRT(C5*C5+C6*C6)*AL(I)
    TSPEC(N)=SIGMA(N)**2*UAS(IK)
    TVAR(N)=TVAR(N)+TSPEC(N)
    TM2(N)=TM2(N)+TSPEC(N)*WS
    TM4(N)=TM4(N)+TSPEC(N)*WS*WS
C   PRINT 131,ALP(I),BET(I),X,C3,C4,C5,C6,AL(I),WE(I),SIGMA(N),,
1150 CONTINUE
1200 N=N+1
    KF(I)=N
    NJD=N-JD-1
    LT(N)=LS(I)+LT(NJD)
    UA(N)=SQRT(B(JK)*B(JK)+B(JJ)*B(JJ))
    VSPEC(N)=WS*UA(N)**2*UAS(IK)
    VVAR(N)=VVAR(N)+VSPEC(N)
    IF (NKK.EQ.0) GO TO 1810
    USPEC(N)=UA(N)**2*UAS(IK)
    UVAR(N)=UVAR(N)+USPEC(N)
    C3=B(JI)*ALP(I)+B(JH)*BET(I)
    C4=-B(JI)*BET(I)+B(JH)*ALP(I)
    C5=C4-QE(I)*C3
    C6=C3+QE(I)*C4
    EBSILO(N)=SQRT(C3*C3+C4*C4)
    ESPEC(N)=EBSILO(N)**2*UAS(IK)
    EVAR(N)=EVAR(N)+ESPEC(N)
    SIGMA(N)=SQRT(C5*C5+C6*C6)*AL(I)
    TSPEC(N)=SIGMA(N)**2*UAS(IK)
    TVAR(N)=TVAR(N)+TSPEC(N)
    TM2(N)=TM2(N)+TSPEC(N)*WS
    TM4(N)=TM4(N)+TSPEC(N)*WS*WS
C   PRINT 131,ALP(I),BET(I),X,C3,C4,C5,C6,AL(I),WE(I),SIGMA(N),,
1810 N=N+1
    LT(N)=LT(N-1)+LP(I)
1100 CONTINUE
    IF (NKK.EQ.0) GO TO 1820
4010 NH=N-1
    PRINT 60, F(IK)
60 FORMAT (1H,//////////* THIS IS THE RESULTS WITH DAMPING AT FREQ
    UE=CY*,F8.6////////9X,UA*,10X,USPEC*,10X,EBSILO*,9X,ESPEC*,10X,
    SIGMA*,10X,TSPEC*,12X,LI*,13X,I*)
    PRINT 70, (UA(I),USPEC(I),EBSILO(I),ESPEC(I),SIGMA(I),TSPEC(I),LI(
    I),I, I=1,NH)
70 FORMAT(7E15.4,110)
1820 KEK=KF(K)
C   PRINT 135, (UA(J),VSPEC(J),VVAR(J),LT(J), J=1,NEN)
135 FORMAT(4E14.4)
2000 CONTINUE
C   PRINT 132, (VVAR(J), LT(J), J=1,KEK)
132 FORMAT (2E14.4)
C   PRINT 133, (KI(J),KE(J), J=1,K)
133 FORMAT (2I10)
    IF (NKK.EQ.0) GO TO 188
    DO 2010 I=1,NH
        TM4=TVAR(I)*TM4(I)
        TM2=TM2(I)*TM2(I)

```

```

      IEB = (1404-1422)/1404
      IEB(I) = SQRT(IEB)
2010 CONTINUE
      PRINT 83,
      FORMAT (1H1,*, UVAR,*,*, EVAR,*,*, IVAR,*,*,
      1*, I=2,*,*, I=4,*,*, IEB*,15X,*1*)
      PRINT 83,(UVAR(I),EVAR(I),IVAR(I),I=2(I),I=4(I),IEB(I),I=1,NI)
      FORMAT (6E15.4,I10)
128 JAP = 0.
      DCR = 0.
      JAP(K) = 1.
      DO 204 I=1,K
      KK=K-I
      JJ=I-E(I)
      JK=JJ-1
      VIAR(I)=0.
      VSAR(I)=0.
      UAPC(I) = SQRT(VVAR(JJ))
      JAPD(I) = UAPC(I)/JAP(I)-1.
      JAPD(K) = 0.
      DO 203 J=KK,JK
      DLT = LT(J+1)-LT(J)
      VJAK(I) = VSAR(I) + VVAR(J)*DLT
      VIAR(I) = VIAR(I) + VVAR(J)**1.5*DLT
      PRINT 136,VVAR(J),VSAR(I),VIAR(I),DLT
136 FORMAT (4F14.4)
202 CONTINUE
      DCRD(I) = VIAR(I)/VSAR(I)
      DCRD(I) = DCRD(I)/DCR(I)-1.
      JAPS = JAPS + JAPD(I)**2
      DCRS = DCRS + DCRD(I)**2
204 CONTINUE
      PRINT 55, DCRS, JAPS
55 FORMAT (1H,*, DCRS=*,E12.4,*, JAPS=*,E12.4//3X,*,VJAK(I)*,5X,*,
      1IAR(I)*,5X,*,DCRD(I)*,5X,*,JAPD(I)*,5X,*,DCRC(I)*,5X,*,UAPC(I)*,5X,*,DC
      1R(I)*,5X,*,UAP(I)*,*, I*)
      PRINT 56,(VJAK(I),VIAR(I),DCRD(I),JAPD(I),DCRC(I),UAPC(I),DCR(I),J
      1AP(I),I=1,K)
56 FORMAT(6E12.4,I5)
      IF (NKK.EQ.1) GO TO 6000
      NIT=NIT+1
      DO 65 I=1,K
      DCR(I) = DCRD(I)
      JAP(I) = JAPC(I)
65 CONTINUE
C
C      ALLOWABLE ERRORS FOR DCRS AND JAPS ARE 0.02%
C
      ERRE = 0.02*FLOAT(K)
      IF (DCRS.GT.ERRE) GO TO 62
      IF (JAPS.GT.ERRE) GO TO 5100
62 IF (NIT.GE.6) GO TO 6000
      GO TO 2001
5000 NKK=1
      GO TO 2001
6000 CONTINUE

```

```

      STOP
      END
      SUBROUTINE INVR(A,N,B,M,DETERM,ISIZE,JSIZE)
      DIMENSION IPIVOT(100),A(ISIZE,JSIZE),B(ISIZE,M),INDEX(100,2),
      IPIVOT(100)
      EQUIVALENCE (IROW,JROW),(ICOLUMN,JCOLUMN),(AMAX,T,SWAP)
C
C   10 DETERM=1.0
C   15 DO 20 J=1,N
C   20 IPIVOT(J)=0
C   30 DO 550 I=1,N
C
C   SEARCH FOR PIVOT ELEMENT
C
C   40 AMAX=0.0
C   45 DO 105 J=1,N
C   50 IF (IPIVOT(J)-1) 60,505.60
C   60 DO 100 K=1,N
C   70 IF (IPIVOT(K)-1) 80,1 0.740
C   80 IF (ABS(AMAX)-ABS(A(J,K))) 85,100,100
C   85 IROW=J
C   90 ICOLUMN=K
C   95 AMAX=A(J,K)
C  100 CONTINUE
C  105 CONTINUE
C  110 IPIVOT(ICOLUMN)=IPIVOT(ICOLUMN)+1
C
C   INTERCHANGE ROWS TO PUT PIVOT ELEMENT ON DIAGONAL
C
C  130 IF (IROW-ICOLUMN) 140, 260, 140
C  140 DETERM=-DETERM
C  150 DO 200 L=1,N
C  160 SWAP=A(IROW,L)
C  170 A(IROW,L)=A(ICOLUMN,L)
C  200 A(ICOLUMN,L)=SWAP
C  205 IF(M) 260, 260, 210
C  210 DO 250 L=1,M
C  220 SWAP=B(IROW,L)
C  230 B(IROW,L)=B(ICOLUMN,L)
C  250 B(ICOLUMN,L)=SWAP
C  260 INDEX(1,1)=IROW
C  270 INDEX(1,2)=ICOLUMN
C  310 PIVOT(1)=A(ICOLUMN,ICOLUMN)
C  320 DETERM=DETERM*PIVOT(1)
C
C   DIVIDE PIVOT ROW BY PIVOT ELEMENT
C
C  330 A(ICOLUMN,ICOLUMN)=1.0
C  340 DO 350 L=1,N
C  350 A(ICOLUMN,L)=A(ICOLUMN,L)/PIVOT(1)
C  355 IF(M) 380,380,360
C  360 DO 370 L=1,M
C  370 B(ICOLUMN,L)=B(ICOLUMN,L)/PIVOT(1)
C
C   REDUCE NON-PIVOT ROWS
C

```

```

380 DO 390 L=1,N
390 IF (L=ICOLUM) 400,550,460
400 T=A(L,ICOLUM)
420 A(L,ICOLUM)=0.0
430 DO 450 L=1,N
450 A(L,L)=A(L,L)-A(ICOLUM,L)*T
455 IF(M)550,550,460
460 DO 500 L=1,M
500 B(L,L)=B(L,L)-B(ICOLUM,L)*T
550 CONTINUE

```

```

C
C   INTERCHANG COLUMNS
C

```

```

600 DO 710 I=1,N
610 L=N+1-I
620 IF (INDEX(L,1)-INDEX(L,2))630,710,630
630 JROW=INDEX(L,1)
640 JCOLUM=INDEX(L,2)
650 DO 705 K=1,N
660 SWAP=A(K,JROW)
670 A(K,JROW)=A(K,JCOLUM)
700 A(K,JCOLUM)=SWAP
705 CONTINUE
710 CONTINUE
740 RETURN
END

```

# EXAMPLE OF DATA INPUT

```

1      3
72000000.    0.    4000000.    30.    1.5    .142    2.    4.    4.5    .27    0
72000000.    0.    4000000.    8850.    1.5    .142    2.    4.    4.5    .27    0
72000000.    0.    4000000.    210.    1.5    .142    2.
18
.01 .03 .05 .07 .09 .11 .13 .15 .17 .19 .21 .23 .25 .27 .29 .31 .33 .35
70. 1000. 1000. 0.0065 1
34.91      .95
34.95 26.54 0.06

```



# REFERENCES

1. Casarella, M. J. and Parson, M., "Cable Systems Under Hydrodynamic Loading," Journ. of Marine Technology Society, Vol. 4, No. 4, July-August 1970.
2. Paquette, R. G. and B. E. Henderson, "Dynamics of Simple Deep-Sea Moorings," Technical Report 65-79, General Motors Defense Research Laboratory, 1965.
3. Wilson, B. W. and D. H. Garbaccio, "Dynamics of Ship Anchor Lines in Waves and Currents," Journal of the Waterways and Harbors Division, ASCE, Vol. 95, No. WW4, Proc. Paper 6888, November 1969, pp. 449-465.
4. Reid, R. O., "Dynamic of Deep Sea Mooring Lines," Technical Report Ref. 68-11f. Texas A & M University, July 1968.
5. Kaplan, P. and Raif, A. I., "Development of a Mathematical Model for a Moored Buoy System," Technical Report No. 69-61, Oceanics, Inc., April 15, 1969.
6. Nath, J. H., "Analysis of Deep Water Single Point Moorings," Technical Report CER 70-71 JHN4, Colorado State University, August 1970.
7. Brainard, J. P., "Dynamic Analysis of a Single Point, Taut, Compound Mooring," Technical Report Ref. No. 71-42, Woods Hole Oceanographic Institute, June 1971. (Unpublished manuscript)
8. Nath, J. H., "Dynamics of Single Point Ocean Moorings of a Buoy - A Numerical Model for Solution by Computer," Progress Report Ref. 69-10, Department of Oceanography, Oregon State University, July 1969.
9. Borgman, L. E., "Ocean Wave Simulation for Engineering Design," Proceedings of the Conference on Civil Engineering in the Oceans, San Francisco 1967.

10. Rice, S. O., "Mathematical Analysis of Random Noise," Bell System Technical Journal, Vols. 23 and 24, 1944.
11. Cartwright, D. E. and Louguett-Higgins, M. S., "The Statistical Distribution of the Maxima of a Random Function," Proceedings of the Royal Society, 1956.
12. Pode, L., "An Experimental Investigation of the Hydrodynamic Forces on Stranded Cable," David Taylor Model Basin, U. S. Navy, May 1950.
13. Wilson, B. W., "Characteristics of Anchor Cable in Uniform Ocean Currents," Technical Report, Texas A. & M. University.
14. Schlichting, H., "Boundary-Layer Theory," McGraw-Hill, 1968.
15. Carslaw, H. S. and Jaeger, J. C., "Operational Methods in Applied Mathematics," Dover, p. 125.
16. Nath, J. H., "An Experimental Study of Wind Forces on Offshore Structures," Technical Report. CER 70-71 JHN3, Colorado State University, August 1970.
17. Davenport, A. G., "Rationale for Determining Design Wind Velocity," ASCE Transactions, Vol. 126, Part II, 1961.
18. Hoerner, S. F., "Fluid Dynamic Drag," published by the author, Midland Park, New Jersey, 1958.
19. Mercier, J. A., "Hydrodynamic Forces on Some Float Forms," Report SIT-DL-69-1407, Davidson Laboratory, Stevens Institute of Technology, October 1969.
20. Gaul, R. D. and Brown, N. L., "A Comparison of Wave Measurements from a Free-Floating Wave Meter and the Monster Buoy," Transactions, Second International Buoy Technology Symposium, Washington D. C. 1967, pp. 473-494.
21. Minorsky, N., "Introduction to Non-Linear Mechanics," Edwards Brothers, Inc. Ann Arbor, Michigan, 1947.